Multiobjective Optimization Under Uncertainty of the Economic and Life-Cycle Environmental Performance of Industrial Processes

Nagore Sabio, Carlos Pozo, Gonzalo Guillén-Gosálbez, and Laureano Jiménez
Departament d'Enginyeria Química, Universitat Rovira i Virgili, 43007 Tarragona, Spain

Ramkumar Karuppiah, Venkatesh Vasudevan, Nicolas Sawaya, and John T. Farrell
Corporate Strategic Research, ExxonMobil Research and Engineering, Annandale, NJ 08801

DOI 10.1002/aic.14385
Published online March 1, 2014 in Wiley Online Library (wileyonlinelibrary.com)

The combined use of multiobjective optimization and life-cycle assessment (LCA) has recently emerged as a useful tool for minimizing the environmental impact of industrial processes. The main limitation of this approach is that it requires large amounts of data that are typically affected by several uncertainty sources. We propose herein a systematic framework to handle these uncertainties that takes advantage of recent advances made in modeling of uncertain LCA data and in optimization under uncertainty. Our strategy is based on a stochastic, multiobjective, and multiscenario mixed-integer nonlinear programming approach in which the uncertain parameters are described via scenarios. We investigate the use of two stochastic metrics: (1) the environmental impact in the worst case and (2) the environmental downside risk. We demonstrate the capabilities of our approach through its application to a generic complex industrial network in which we consider the uncertainty of some key life-cycle inventory parameters. © 2014 American Institute of Chemical Engineers *AIChE J*, 60: 2098–2121, 2014
Keywords: multiobjective optimization, life-cycle assessment, uncertainty

Introduction

Over the past few years, there has been a significant amount of research in both academia and industry on incorporating environmental aspects in traditional process design and optimization, in addition to economic criteria. This paradigm shift in the scope of the analysis has been motivated by several drivers, such as the establishment of more stringent environmental regulations. As a result, new tools are continuously being developed to assist with the systematic generation and assessment of process alternatives that could enable environmental improvements.[1]

Among them, life-cycle assessment[2] (LCA) has recently gained wider interest in the research community. In essence, LCA adopts a holistic approach that accounts for all the inputs (mass and energy) and outputs (emissions and waste) of a process over its entire life cycle. LCA studies are, therefore, mostly based on a cradle-to-grave analysis that covers the most relevant activities associated with a process, including raw material extraction, manufacture of a product, use of the product, and its end-of-life treatment.

Current address of V. Vasudevan: ExxonMobil Chemical Company, Houston, TX 77079
Current address of N. Sawaya: ExxonMobil Gas & Power Marketing, Houston, TX 77002
Current address of J. Farrell: National Renewable Energy Laboratory, Golden, CO 80401

Correspondence concerning this article should be addressed to G. Guillén-Gosálbez at gonzalo.guillen@urv.cat.

LCA was initially conceived as a descriptive tool for assessing environmental performance and pinpointing the main sources of impact in a process or product life cycle. The lack of systematic analyses to improve environmental performance represents a major shortcoming of conventional LCA studies and tools since guidelines on how to achieve improvements are not available. Azapagic and Clift[3] were the first to propose the integration of LCA and multiobjective optimization (MOO) as an effective method to overcome this limitation and expand the capabilities of LCA tools. This combined approach automates the search for alternatives with better life-cycle environmental performance, some of which may be nonintuitive or hard to identify using traditional tools. Treating environmental impacts as additional objectives rather than as constraints in the system has the additional advantage of avoiding articulation of the decision-makers' preferences prior to the optimization step. This may lead to solutions where significant environmental benefits are attained at a marginal decrease in economic performance.

In recent years, the combined use of MOO and LCA has expanded rapidly in both academia and industry, finding applications in a wide variety of problems including the design of chemical plants[4]; the design and scheduling of batch processes[5]; the selection of solvents in mass separating agent driven technologies[6]; the design of utility systems[7,8]; the design of absorption cooling cycles[9,10]; the design of polygeneration energy systems[11]; the design of chemical supply chains[12–16]; and the strategic planning of hydrogen supply chains[17,18] and supply chains for ethanol production,[19,20]

among others. The reader is referred to the review article by Pieragostini et al.[21] for further examples on this topic.

Yet, one major limitation of MOO models that integrate LCA principles is that they rely on deterministic formulations that assume that all model parameters are perfectly known in advance and show no variability.[1] These models focus on analyzing the system in the most likely scenario, assuming that the impact will not differ from the one predicted under nominal conditions. In practice, however, there are many sources of uncertainty in the LCA calculations, which typically stem from imprecise measurements or lack of data. Neglecting these uncertainties may lead to solutions with good performance on average, but with large probabilities of not meeting the desired environmental targets.

Optimization under uncertainty has recently attracted a growing interest in the process systems engineering (PSE) community (see for instance Sahinidis[22] for general references on this topic, and Aseeri and Bagajewicz[23] for more specific methods for risk management under uncertainty in the PSE literature). Substantial research has focused on uncertainties in demand, prices, yields, and operating times, but very little work has addressed the MOO of process industries considering uncertainties in their life-cycle environmental assessment. Uncertainties in LCA data, in contrast, have been in the research agenda of the LCA community for quite a long time. The emphasis in previous work has been placed on understanding how these uncertainties affect the outcome of the LCA rather than on identifying robust solutions that minimize their effects.

In a previous work, Heijungs[24] presented a general taxonomy that distinguished between variability and uncertainty in LCA studies. The first is understood as stemming from inherent variations in the real world (e.g., spatial and temporal variability), while uncertainty comes from inaccurate measurements, lack of data, and model assumptions associated with the LCA calculations. Uncertainty in LCA can be further divided into parameter uncertainty, model uncertainty, and uncertainty due to choices. In contrast, variability covers spatial variability, temporal variability, and variability between objects and sources. The combination of different formalisms to deal with uncertainty and variability simultaneously poses significant mathematical challenges and might not result in a theoretically sound approach.[25] Hence, different tools need to be devised according to the uncertainty source. Particularly, in this work, we focus on uncertainties in the life-cycle inventory (LCI), which typically constitute the main source of uncertainty in LCA studies.

Uncertainty analysis and sensitivity analysis are the two main methods to handle uncertainties in LCA. The former provides a full description on how the uncertain parameters affect the LCA outcome. It comprises two steps: a first phase in which the LCA inputs are modeled and a second step in which uncertainties are propagated through the LCA calculations. Conversely, sensitivity analysis is a simpler strategy that studies the effects that arbitrary changes in some LCA inputs have on the LCA outputs. This technique allows identification of the most influential LCA inputs in cases in which uncertainty quantification is difficult. Although no method is in principle superior, the first is preferred when comparing product/process alternatives,[25] which makes it better suited for optimization under uncertainty.

A key issue in uncertainty analysis is the characterization of the uncertain parameters. The main approaches proposed to address these include analytical uncertainty propagation techniques,[24,26] uncertainty intervals,[27] fuzzy logic,[28] Bayesian statistics,[29] and stochastic modeling.[30] Among them, stochastic modeling is particularly appealing because it can handle various parameter distributions while simultaneously accounting for correlations between them. In stochastic modeling, the uncertain parameters are described by means of uncertainty distributions (e.g., normal, log-normal, etc.) from which random values (restricted within the limits of the distribution) are generated using sampling methods. In essence, this technique repeats the LCA calculations for every potential outcome of the random variables, obtaining a set of values that are used to construct distributions of the LCI and life-cycle impact assessment (LCIA) results.

Stochastic modeling has found many applications in LCA. Capello et al.[31] applied this method for generating reliable data ranges for inventory flows of waste solvent distillation. Geisler et al.[32] assessed the uncertainty associated with the LCI flows and characterization factors of two pesticides using Monte Carlo simulation. Sugiyama et al.[33] proposed a procedure for incorporating uncertainty information with statistical methods in industry-based LCI databases. Van Zelm et al.[34] quantified uncertainties in freshwater ecotoxicological effect factors for several pesticides using Monte Carlo sampling. Hung and Ma[35] proposed also a methodology based on Monte Carlo simulation to systematically analyze the uncertainties involved in the entire LCA methodology (i.e., LCI, LCIA, and the normalization and weighting parameters) and applied it to a set of municipal solid waste management strategies in Taiwan.

Despite these advances in LCA, the overwhelming majority of the approaches that integrate MOO and LCA principles are based on deterministic formulations that assume that all model parameters are perfectly known in advance[36] (i.e., they are deterministic and show no variability). These models might produce solutions with good performance in the most likely scenario, but which can have large probabilities of impacts above the desired target limits.

To the best of our knowledge, Guillén-Gosálbez and Grossmann[37,38] were the first to present a systematic tool based on mathematical programming for the minimization of the LCA impact under uncertainty in the LCI and LCIA parameters. They introduced a robust optimization framework that allows definition of probabilistic targets for the environmental impacts using chance constraints. This approach relies on the strong assumption that all uncertain parameters follow normal uncorrelated distributions. In conventional LCA studies, however, uncertain parameters can follow other distributions (such as uniform, triangular, or log-normal), and some of them might be correlated.

We propose herein a systematic method to handle LCA uncertainties in MOO that overcomes the limitations aforementioned. Our approach, which makes no assumption concerning the underlying probability functions, relies on a multiscenario stochastic optimization model in which the uncertain parameters are described through scenarios with given probability of occurrence. These scenarios are generated by means of sampling techniques. We assess the use of two stochastic metrics that can be optimized to control the environmental performance under uncertainty, both of which are widely used in financial risk management: the worst case (WC) performance and the downside risk. We demonstrate the capabilities of our approach through its application to a complex industrial network, in which we analyze the uncertainty of the LCI data pertaining to the main feedstock. Hence, the two main novelties of the work are the development of a systematic method for the simultaneous optimization of the economic and life-cycle environmental

performance of industrial processes that explicitly considers the uncertainty associated with the LCI of emissions (without making any assumption on the form of the underlying probability functions), and the application of this systematic approach to a case study based on a generic complex industrial facility. The remainder of this article is organized as follows. We first formally describe the industrial problem of interest and present a mathematical formulation that embeds LCA principles. The stochastic mathematical formulation and an efficient solution procedure that constitute the core of our systematic framework are then described. We then illustrate the capabilities of our approach through its application to a generic complex industrial network. The conclusions of the work are drawn in the last section of the article.

Problem Statement

Superstructure description

We address the optimization of the generic industrial network shown in Figure 1 (Figure 1a depicts the main process, whereas Figure 1b provides details on the utilities consumed and produced by the system), considering both economic and environmental indicators.

The network comprises a set of process units that convert raw materials R1–R4 (shown in Figure 1a) into four main products (products P1–P4, stored in tanks T1–T4, respectively) and three byproducts (P5–P7, stored in tanks T5–T7, respectively). Each stream in the network is characterized by a set of key properties that must lie within some bounds to ensure certain quality specifications imposed on the final products. Streams can be merged and split using mixers and splitters, denoted by blue diamonds and circles, respectively, in Figure 1a. These mixers and splitters also allow the bypassing of some process units, providing the network with flexibility. The operation of each process unit is defined by a set of key process variables (such as temperature and pressure) that can be modified to meet the production targets from the standpoint of quantity and quality. A general description of the network topology follows.

The main feedstock R1 passes through Unit 1 and is subsequently converted to products P1–P4. The output streams leaving Unit 1 are either sent to Units 2, 3, 4, 5, and 7, or directly to the final product storage tanks T1–T4. Units 3, 4, 5, and 7 are used to remove impurities from the output streams exiting Unit 1. Process units consume utilities U1–U7. U1–U4 are fuels used in the process units, while U5, U6, and U7 are steam, electricity, and cooling water. Fuels U1 and U2 can be used simultaneously in any process unit, and the same holds for fuels U3 and U4. Utilities U2 and U4 are produced internally, whereas the rest are purchased from external suppliers. Utility U2 is generated in Unit 7. Utility U4 can be obtained from the gaseous output streams coming from Units 1–9, which are first mixed in a mixer and then purified in Unit 10, as illustrated in Figure 1b. The components removed from these streams are sent to tank T5. The purified stream (utility U4) can either be sold as a byproduct (P7, stored in tank T7) or recycled back to other process units for use as fuel.

Storage tanks T1–T4 merge streams coming from different process units to obtain the desired final products P1–P4. Storage tanks T5–T7 receive streams from different parts of the process network, which can be sold as byproducts. Flow rates of the streams between process units and the process operating conditions can both be modified to meet quality specifications on the final products. Raw materials R1, R2, R3, and R4 can be purchased from external suppliers (i.e., outsourcing), whereas raw material R2 can be recycled from Unit 6, which produces it as a byproduct.

Problem definition

Based on the superstructure described above, we formally state the problem of interest. We are given a set of final products (P1–P4), their corresponding demands in terms of quantity and quality, and economic and environmental data associated with the network operation. The goal is to determine the optimal operating conditions that can optimize simultaneously both economic and environmental performance of the network. One set of decisions includes the operating conditions of the process units as well as stream flow rates. The other set of decisions concerns the selection of a particular fuel in a given process unit. We consider two groups of fuels: fuels U1 and U2, and fuels U3 and U4. U1 can be mixed with U2 and used as fuel, and the same holds for U3 and U4. Fuels belonging to different groups cannot be mixed as each fuel type requires a different unit configuration. The use of U1/U2 precludes the use of U3/U4 in a process unit and vice-versa. Fuels U1 and U3 are purchased from outside, whereas fuels U2 and U4 are recycled from other process units.

Furthermore, we consider that some parameters used in the environmental assessment of the process (i.e., LCI entries) are uncertain and can be described through scenarios (each having a different set of values of the uncertain parameters). These uncertainties in the LCI parameters typically originate from empirical inaccuracy (imprecise measurements), incomplete or outdated measurements, and lack of data (no measurements).

Mathematical Formulation: Deterministic Model

We describe here the deterministic model that is taken in the next section as a basis to develop the stochastic formulation. Hence, to address the problem described in the preceding section, we formulate a mixed-integer nonlinear program (MINLP), in which continuous variables model operating conditions, streams flow rates and economic and environmental performance metrics, while binary variables represent the discrete decisions described previously. This MINLP is based on a high-level representation of the network in which the performance of each process unit is modeled using nonlinear empirical correlations available in the literature. These correlations are used to estimate the properties of output streams and utility consumption rates for the process units, using the properties of the input streams to the units and their operating conditions.

The model is comprised of four main sets of equations: (1) mass-balance constraints; (2) utility consumption constraints; (3) equations describing the operation of the process units; and (4) objective function-related equations that determine economic and environmental performance. We next describe each of these blocks of constraints.

Mass-balance constraints

Mass balances are defined for every process unit of the network. Figure 2 provides a sketch of a generic process unit i, which has a set of input and output streams, denoted by SI_i and SO_i, respectively. For simplicity, in the derivation of

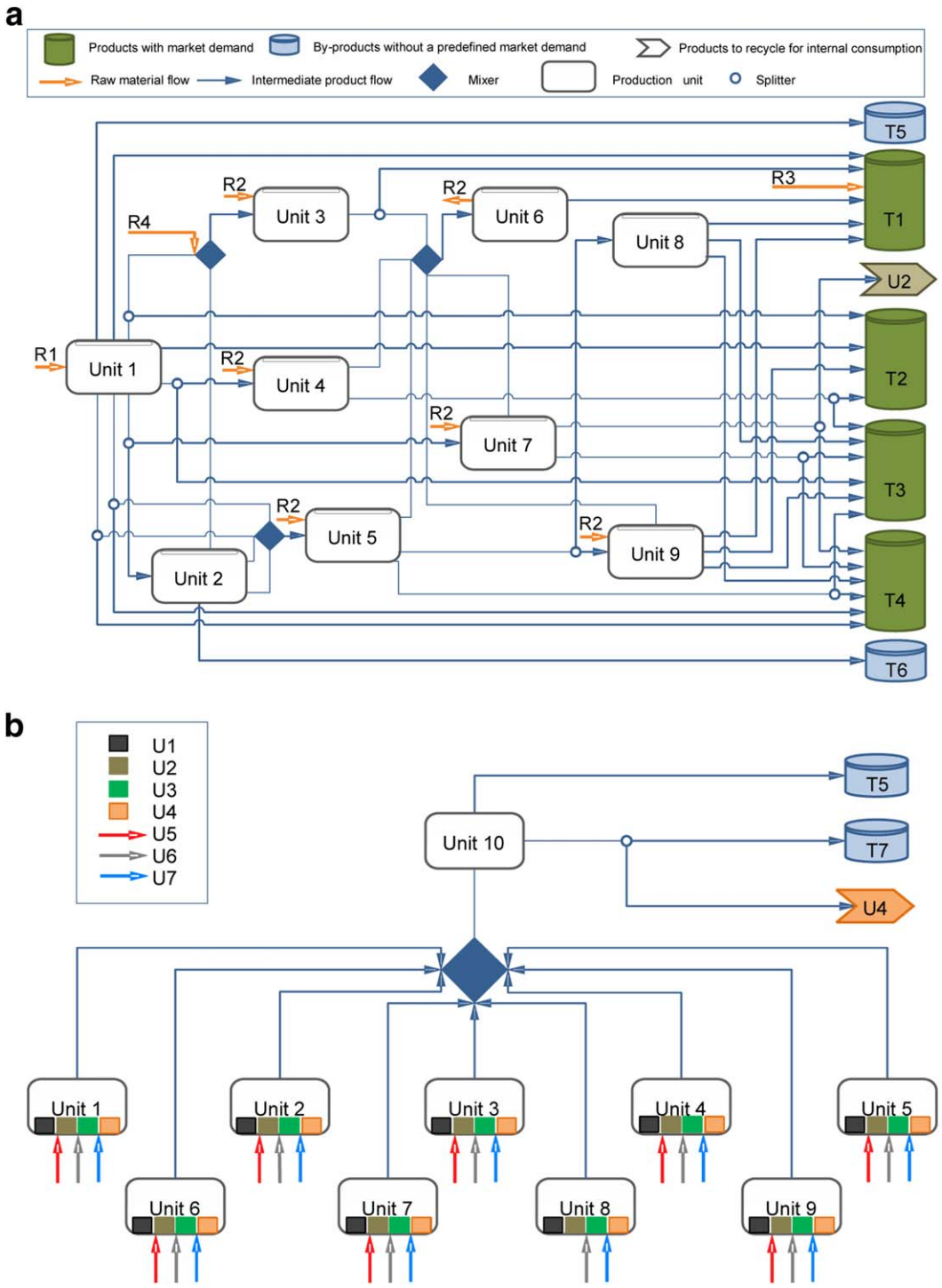

Figure 1. (a) Process network studied.

There are nine process units: four raw materials (one main feedstock R1 and three other raw materials R2, R3, and R4), four final products stored in tanks T1–T4, and three byproducts stored in T5, T6, and T7 (b) and (b) Utilities consumed in the process network. U1–U4 are fuels, while U5, U6, and U7 correspond to steam, electricity, and cooling water, respectively. Gaseous streams coming from the process units are purified in Unit 10, generating fuel U4 and a byproduct stored in tank T5. U4 can be either internally recycled or stored in tank T7 prior to being sold as a byproduct. [Color figure can be viewed in the online issue, which is available at wileyonlinelibrary.com.]

the mass balances, we define for each unit a main input stream. Hence, in Figure 2, MS_i is the main stream into unit i. Most process units have only a single input stream that is treated as the main stream, and several output streams (units Unit 1, Unit 2, Unit 6, and Unit 8). There are others with two input streams (e.g., a main input stream and a secondary input stream containing raw material R2) and several output streams. This is the case in Units 3, 4, 5, 7, and 9.

The mass balance for unit i is expressed via Eq. 1, which states that the total input mass flow rate to each unit must equal the total output mass flow rate

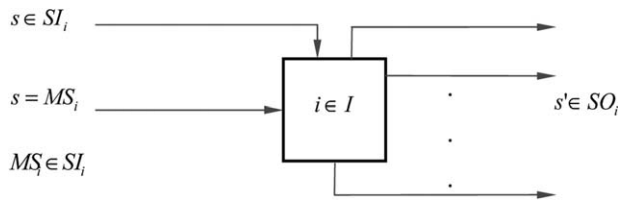

Figure 2. Generic process unit.

$$\sum_{s \in \mathrm{SI}_i} M_s = \sum_{s' \in \mathrm{SO}_i} M_{s'} \quad \forall i \in I \tag{1}$$

In this equation, M_s denotes the mass flow rate of stream s, and SI_i and SO_i represent the set of input and output streams of unit i, respectively.

The output stream flow rates are linked to the main input stream flow rate through the use of yields, which are expressed either on a mass or volume basis. The mass flow rates of the output streams of the units are obtained from Eq. 2, in which MS_i represents the main stream of unit i (recall that $|\mathrm{MS}_i| = 1$), and the continuous variable $\mathrm{YIELD}_{i,s'}^{\mathrm{MASS}}$ denotes the mass yield associated with output stream s' of unit i

$$M_{s'} = M_s \frac{\mathrm{YIELD}_{i,s'}^{\mathrm{MASS}}}{100} \quad \forall i \in IM, \forall s \in \mathrm{MS}_i, \forall s' \in \mathrm{SO}_i \tag{2}$$

Here, IM is the set of units for which mass yields are defined. Note that Eq. 1 is a surrogate of the individual mass balances expressed by Eq. 2 (i.e., Eq. 1 can be obtained by summing up all equations of type (2), so it can be omitted from the model without losing information). Volumetric flow rates are determined using volumetric yields via Eq. 3

$$F_{s'} = F_s \frac{\mathrm{YIELD}_{i,s'}^{\mathrm{VOL}}}{100} \quad \forall i \in IV, \forall s \in \mathrm{MS}_i, \forall s' \in \mathrm{SO}_i \tag{3}$$

In this equation, the continuous variable F_s denotes the volumetric flow rate of stream s, whereas the continuous variable $\mathrm{YIELD}_{i,s'}^{\mathrm{VOL}}$ represents the volume basis yield of output stream s' of unit i. IV is the set of units for which volume yields are defined.

The relationship between mass and volume flow rates is given in Eq. 4, in which GR_s represents the density of stream s

$$M_s = F_s \mathrm{GR}_s \quad \forall \mathrm{s} \in \mathrm{S} \tag{4}$$

The amount of R2 consumed by process units 3, 4, 5, 7, and 9 is determined from the volumetric flow rate of the main input stream (variable F_s) and the continuous variable $\mathrm{RMCONS}_i^{\mathrm{VOL}}$ via Eq. 5

$$F_{s''} = F_s \frac{\mathrm{RMCONS}_i^{\mathrm{VOL}}}{100} \quad \forall i \in IR, \forall s \in \mathrm{MS}_i, \forall s'' \in \mathrm{SI}_i, \forall s'' \notin \mathrm{MS}_i \tag{5}$$

Here, IR is the set of units consuming R2. The consumption rate of R2 can also be determined on a mass basis via Eq. 6, where continuous variable $\mathrm{RMCONS}_i^{\mathrm{MASS}}$ links the mass flow rate of R2 to that of the main input stream

$$M_{s''} = M_s \frac{\mathrm{RMCONS}_i^{\mathrm{MASS}}}{100} \quad \forall i \in IR, \forall s \in \mathrm{MS}_i, \forall s'' \in \mathrm{SI}_i, \forall s'' \notin \mathrm{MS}_i \tag{6}$$

Capacity limitations that impose upper bounds on the total input flow rate to each process unit are given in Eq. 7

$$\sum_{s \in \mathrm{SI}_i} M_s \leq \mathrm{CAP}_i^{\mathrm{MASS}} \quad \forall i \in I \tag{7}$$

Here, parameter $\mathrm{CAP}_i^{\mathrm{MASS}}$ denotes the mass flow rate capacity of unit i. Note that usually industrial processes might have also a lower bound regarding their operability region. This is to avoid solutions with very low flows, which may be impractical for standard equipment sizes. This lower bound could be also enforced through an inequality similar to Eq. 7. Equation 7 can also be expressed on a volume basis as follows

$$\sum_{s \in \mathrm{SI}_i} F_s \leq \mathrm{CAP}_i^{\mathrm{VOL}} \quad \forall i \in I \tag{8}$$

Where parameter $\mathrm{CAP}_i^{\mathrm{VOL}}$ represents the capacity of unit i on a volumetric flow basis.

Utility consumption constraints

Utilities U1–U4 are fuels used to power the process units. Utilities U5, U6, and U7 represent steam, electricity, and cooling water. The total amount of utility u consumed by a process is denoted by the continuous variable TCONS_u, which is determined from the consumption rates of each unit and the total number of operating hours, as stated in Eq. 9

$$\mathrm{TCONS}_u = \sum_{i \in I_u} \mathrm{UTCONS}_{i,u} \mathrm{TOP} \quad \forall u \in U \tag{9}$$

In this equation, $\mathrm{UTCONS}_{i,u}$ is a continuous variable denoting the consumption rate of utility u in unit i, TOP is a parameter that represents the total number of operating hours, and I_u is the set of process units that consume utility u. Constraint (10) determines the consumption rate in every unit (represented by variable $\mathrm{UTCONS}_{i,u}$) for utilities other than fuels

$$\mathrm{UTCONS}_{i,u} = F_s \mathrm{UTRATE}_{i,u} \quad \forall i \in I, \forall s \in \mathrm{MS}_i, \forall u \in U_i, \mathrm{u} \neq U1, U2, U3, U4 \tag{10}$$

Here, $\mathrm{UTRATE}_{i,u}$ is a mass-balance coefficient that links the amount of utility u consumed by unit i to the flow rate of the main input stream, while U_i is the set of utilities consumed by unit i.

Equation 11 applies to fuels. As aforementioned, the model assumes that each process unit can operate with either U1/U2 or U3/U4. To calculate the amount of each fuel consumed by unit i, we proceed as follows. We first determine the energy consumption of the unit by multiplying the volumetric flow rate (continuous variable F_s) of the main input stream ($s \in \mathrm{MS}_i$) by an energy consumption factor that is defined for every unit (parameter ECONS_i). The total energy demand of the unit is equal to the summation of the consumption rates of every fuel in that unit

$$F_s \mathrm{ECONS}_i = \sum_{u = U1, U2, U3, U4} \mathrm{UTCONS}_{i,u} \quad \forall i \in I, \forall s \in \mathrm{MS}_i \tag{11}$$

Because simultaneous use of fuels of different types is disallowed, we introduce binary variable Y_i that equals 1 if

fuels of Type 1 (i.e., U1 and U2) are selected in unit i, and zero otherwise (i.e., if either U3 or U4 is used).

The definition of Y_i is enforced via Eqs. 12 and 13. These constraints work as follows. If the first pair of fuels is selected, then the binary variable will take the value of 1 ($Y_i=1$). Equation 13 will then make the consumption rates of U3 and U4 equal to zero, whereas Eq. 12 will allow the consumption rates of U1 and U2 to take on any value between zero and an upper bound BM. Note that constraint (11) will ensure that the amount of U1 and U2 consumed is sufficient to cover the energy needs of the unit. Conversely, if fuels U1 or U2 are not selected, the binary variable will be zero, and Eq. 12 will force their consumption rates to zero, whereas constraint (13) will allow the consumption rates of U3 and U4 to lie between zero and the upper bound BM. Equation 11 will again ensure that the energy needs of the unit are fully satisfied through the use of U3 and U4

$$\mathrm{UTCONS}_{i,u} \le \mathrm{BM}(Y_i) \quad \forall i \in I, u=U1, U2 \tag{12}$$

$$\mathrm{UTCONS}_{i,u} \le \mathrm{BM}(1-Y_i) \quad \forall i \in I, u=U3, U4 \tag{13}$$

In these equations, BM must be carefully set to avoid poor numerical performance while also guaranteeing that the energy requirements of each process unit can be fully met.

Process units

Process units are modeled using tailored correlations that determine the properties, yields, and consumption rates of output streams using properties, process operating conditions, and raw material consumption rates of input streams. These correlations, which are empirical, comprise a set of nonlinear equations that follow no predefined pattern and that contain four main types of continuous variables: variable $\mathrm{OPC}_{i,o}$ denotes the value of operating condition o in process unit i; variable $\mathrm{PROP}_{s,p}$ is the value of property p in stream s; $\mathrm{YIELD}_{i,s}$ is the yield of stream s exiting unit i expressed either on a volume or mass basis; and $\mathrm{RMCONS}_{i,s}$ is the flow rate of stream s entering unit i.

Process correlations are represented by general mathematical functions $f^i_y(\cdot)$, in which i indicates the unit being modeled by the correlation and y denotes either a property of a stream, an operating condition, a yield, or a consumption rate. The specific structure of these functions depends on the unit being modeled. For simplicity and also due to space limitations, we will present them generically without getting into the details of their specific form.

Operating conditions are modeled as either parameters or decision variables depending on the process unit. These are a function of other operating variables and stream properties, as shown in Eq. 14

$$\begin{aligned}&\mathrm{OPC}_{i,o}=f^i_{\mathrm{OPC}_{i,o}}(\mathrm{OPC}_{i,o'}, \mathrm{PROP}_{s,p})\\ &\forall i \in I, \forall o, o' \in OI_i, \forall p \in \mathrm{PS}_s, \forall \mathrm{s} \in \{\mathrm{SI}_i \cup \mathrm{SO}_i\}\end{aligned} \tag{14}$$

In Eq. 14, OI_i represents the set of operating conditions defined for unit i and PS_s the set of properties defined for stream s, which belongs to the set of streams entering and exiting unit i.

Yields are determined using operating conditions, streams properties, raw materials consumption rates, and other yields, as shown in Eq. 15

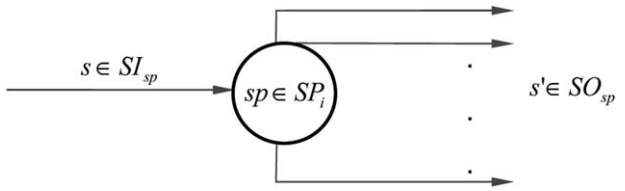

Figure 3. Splitter.

$$\begin{aligned}&\mathrm{YIELD}_{i,s}=f^i_{\mathrm{YIELD}_{i,s}}(\mathrm{OPC}_{i,o}, \mathrm{PROP}_{s',p}, \mathrm{RMCONS}_{i,s''}, \mathrm{YIELD}_{i,s'''})\\ &\forall i \in I, \forall o \in OI_i, \forall p \in \mathrm{PS}_{s'}, \forall \mathrm{s}, \forall s''' \in \mathrm{SO}_i \forall s' \in \{\mathrm{SI}_i \cup \mathrm{SO}_i\},\\ &\forall s'' \in \mathrm{SI}_i, \forall s'' \notin \mathrm{MS}_i\end{aligned} \tag{15}$$

Similarly, raw materials consumption rates are determined using operating conditions, stream properties, and yields using Eq. 16

$$\begin{aligned}&\mathrm{RMCONS}_{i,s}=f^i_{\mathrm{RMCONS}_{i,s}}(\mathrm{OPC}_{i,o}, \mathrm{PROP}_{s',p}, \mathrm{YIELD}_{i,s''})\\ &\forall i \in I, \forall o \in OI_i, \forall p \in \mathrm{PS}_{s'}, \forall \mathrm{s} \in \mathrm{SI}_i, \forall s \notin \mathrm{MS}_i,\\ &\forall s' \in \{\mathrm{SI}_i \cup \mathrm{SO}_i\}, \forall s'' \in \mathrm{SO}_i\end{aligned} \tag{16}$$

Stream properties are determined using operating conditions, other stream properties, raw materials consumption rates, and yields, as shown in Eq. 17

$$\begin{aligned}&\mathrm{PROP}_{s,p}=f^i_{\mathrm{PROP}_{s,p}}(\mathrm{OPC}_{i,o}, \mathrm{PROP}_{s',p'}, \mathrm{RMCONS}_{i,s''}, \mathrm{YIELD}_{i,s'''})\\ &\forall i \in I, \forall o \in OI_i, \forall p \in \mathrm{PS}_s, \forall p' \in \mathrm{PS}_{s'}, \forall s, s' \in \{\mathrm{SI}_i \cup \mathrm{SO}_i\},\\ &\forall s'' \in \mathrm{SI}_i, \forall s'' \notin \mathrm{MS}_i, \forall s''' \in \mathrm{SO}_i\end{aligned} \tag{17}$$

Splitters

Splitters divide a given input stream flow into several output streams. Figure 3 depicts a generic representation of a splitter sp, where SP_i is the set of splitters whose input stream comes from unit i, SI_{sp} denotes the set of input streams of splitter sp (whose cardinality is one), and SO_{sp} is the set of output streams from splitter sp.

The mass balance states that the sum of the output mass flow rates must equal the input mass flow rate, as enforced by Eq. 1.

The properties of the output streams are assumed to be the same as the properties of the input streams, as shown in Eq. 18

$$\begin{aligned}&\mathrm{PROP}_{s,p}=\mathrm{PROP}_{s',p}\\ &\forall i \in I, \forall p \in \mathrm{PS}_s, \forall sp \in \mathrm{SP}_i, \forall s \in \mathrm{SI}_{sp}, \forall s' \in \mathrm{SO}_{sp}\end{aligned} \tag{18}$$

Mixers

Mixers merge several streams into a single output (see Figure 4). The output stream mass flow rate should be the sum of the mass flow rates of the input streams. This condition is enforced via Eq. 1.

In the description of mixers, we make use of the following sets: MX_i, which represents the set of mixers associated with unit i (i.e., those mixers whose output stream goes to unit i), $\mathrm{SI}_{\mathrm{mx}}$, which represents the set of input streams of mixer mx, and $\mathrm{SO}_{\mathrm{mx}}$, which denotes the output stream of mixer mx (whose cardinality is one).

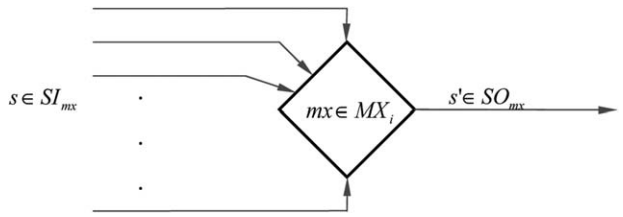

Figure 4. Mixer.

Most output stream properties are determined as a weighted average of the same property in the input streams. The weights can be expressed either on a volume or mass basis (Eqs. 19 and 20). In some cases, the output property is calculated using the inverse of the input property (Eq. 21). In addition, certain properties are determined using tailored correlations (Eq. 22)

$$\sum_{s\in \mathrm{SO}_{\mathrm{mx}}} F_s \mathrm{PROP}_{s,p} = \sum_{s'\in \mathrm{SI}_{\mathrm{mx}}} F_{s'} \mathrm{PROP}_{s',p} \quad \forall i \in I, \forall \mathrm{mx} \in MX_i, \forall p \in \mathrm{PV} \tag{19}$$

$$\sum_{s\in \mathrm{SO}_{\mathrm{mx}}} M_s \mathrm{PROP}_{s,p} = \sum_{s'\in \mathrm{SI}_{\mathrm{mx}}} M_{s'} \mathrm{PROP}_{s',p} \quad \forall i \in I, \forall \mathrm{mx} \in \mathrm{MX}_i, \forall p \in \mathrm{PM} \tag{20}$$

$$\sum_{s\in \mathrm{SO}_{\mathrm{mx}}} \frac{F_s}{\mathrm{PROP}_{s,p}} = \sum_{s'\in \mathrm{SI}_{\mathrm{mx}}} \frac{F_{s'}}{\mathrm{PROP}_{s',p}} \quad \forall i \in I, \forall \mathrm{mx} \in \mathrm{MX}_i, \forall p \in \mathrm{PI} \tag{21}$$

$$\mathrm{PROP}_{s,p} = f^{\mathrm{mx}}_{\mathrm{PROP}_{s,p}}(\mathrm{PROP}_{s',p'}) \quad \forall i \in I, \forall \mathrm{mx} \in \mathrm{MX}_i, \forall p \in \mathrm{PT}, \quad \forall p' \in \mathrm{PS}_{s'} \forall \mathrm{s} \in \mathrm{SO}_{\mathrm{mx}}, \forall s' \in \{\mathrm{SI}_{\mathrm{mx}} \cup \mathrm{SO}_{\mathrm{mx}}\} \tag{22}$$

In these equations, PV and PM are the subset of properties calculated using a weighted average expressed on a volumetric or mass basis, respectively; PI denotes the subset of properties determined using the inverse of the properties in the input streams; and PT accounts for the subset of properties obtained via tailored correlations. Note that the left-hand side of Eqs. 19–22 includes only one single term in all the cases.

Storage tanks are modeled as generic mixers. In addition to Eqs. 19–22, we define demand satisfaction (Eq. 23) and product quality constraints (Eq. 24) for these storage tanks. The former ensures that product sales lie within lower and upper bounds. In constraint Eq. 23, DSAT_s is a parameter that represents the minimum demand satisfaction level to be attained (i.e., minimum percentage of the demand, denoted by parameter D_s, to be fulfilled) and SFP is the set of final products

$$D_s \mathrm{DSAT}_s \le F_s \le D_s \quad \forall s \in \mathrm{SFP} \tag{23}$$

Product quality constraints (Eq. 24) impose lower and upper bounds on product properties. This equation uses the set PE, which includes stream properties for which quality specifications are defined, and parameters $\mathrm{PROP}^{\mathrm{LO}}_{s,p}$ and $\mathrm{PROP}^{\mathrm{UP}}_{s,p}$, which define lower and upper bounds for these properties

$$\mathrm{PROP}^{\mathrm{LO}}_{s,p} \le \mathrm{PROP}_{s,p} \le \mathrm{PROP}^{\mathrm{UP}}_{s,p} \quad \forall p \in \mathrm{PE}, \forall s \in \mathrm{SFP} \tag{24}$$

Objective function evaluation

The model seeks to optimize simultaneously the economic performance and environmental impact of the process network. We describe below how we quantify these performance criteria.

Economic Performance. The economic performance, denoted by the continuous variable ECOP, is determined from revenues (REV) and costs (COSTS) using the generic function $g_{\mathrm{ECOP}}(\cdot)$ (Eq. 25)

$$\mathrm{ECOP} = g_{\mathrm{ECOP}}(\mathrm{REV}, \mathrm{COSTS}) \tag{25}$$

Revenues (continuous variable REV) are determined from the sales of final products and byproducts, as stated in Eq. 26

$$\mathrm{REV} = \sum_{j\in J} \sum_{s\in \mathrm{SFP}_j} M_s \mathrm{PRICE}_j \tag{26}$$

In this equation, J is the set of final products and byproducts j, while SFP_j represents the set of product/byproduct streams containing material j. In the same equation, PRICE_j is a parameter that denotes the selling price of product/byproduct j.

The costs term takes into account the cost of raw materials (denoted by continuous variable RMCOSTS) and utilities (denoted by continuous variable UTCOSTS), as indicated in Eq. 27

$$\mathrm{COSTS} = \mathrm{RMCOSTS} + \mathrm{UTCOSTS} \tag{27}$$

Raw material costs are obtained using the amount and price of raw materials consumed as shown in Eq. 28

$$\mathrm{RMCOSTS} = \sum_{k\in K} \left(\sum_{s\in \mathrm{SRMP}_k} M_s - \sum_{s\in \mathrm{SRMR}_k} M_s \right) \mathrm{COST}^{\mathrm{RM}}_k \tag{28}$$

In the above equation, M_s is the mass flow rate of stream s, K is the set of raw materials, SRMP_k denotes the set of streams containing raw material k, and SRMR_k is the set of streams that contain raw material k that is recycled from other process units of the network. $\mathrm{COST}^{\mathrm{RM}}_k$ is a parameter that represents the per unit cost of raw material k.

The cost of utilities, denoted by the continuous variable UTCOSTS, is obtained from the amount of utilities that are purchased externally (all except for U2 and U4 that are recycled) and their corresponding per unit cost, as indicated in Eq. 29

$$\mathrm{UTCOSTS} = \sum_{u\neq U2,U4} \mathrm{TCONS}_u \mathrm{COST}^{\mathrm{UT}}_u \tag{29}$$

In this equation, TCONS_u is the total amount of utility u consumed and parameter $\mathrm{COST}^{\mathrm{UT}}_u$ denotes the per unit cost of utility u. Note that utilities U2 and U4 are obtained from streams coming from other units of the network, so through the general mass-balance equations we make sure that the amount of utilities consumed equals the amount produced (i.e., they have to be produced at the same rate they are consumed).

Environmental Impact. The environmental impact of the industrial network is assessed using the LCA methodology.[2] We combine optimization tools with LCA principles within a unified framework, as done in previous studies.[4,9,10,13–15,18,19] The standard LCA methodology encompasses four main phases that allow quantification of the environmental impact usually from cradle to grave. The main LCA phases, as defined and applied in the current study, are:

1. Phase 1: Goal and scope definition

In this phase, the system boundaries, the environmental impact categories, and the functional unit of the analysis are

defined. We perform a "cradle-to-gate" analysis, where we cover all the steps from the extraction of the necessary raw materials to the point at which the final products become available in the storage tanks. As will be explained in detail later in the case study, the environmental performance is assessed according to three midpoint LCA-based metrics. The functional unit of the study is a given fixed amount of final products P1–P4 (whose demand must be fulfilled).

2. Phase 2: Inventory Analysis

The aim of this phase of the LCA is to identify and quantify the emissions, waste generated, and feedstock requirements associated with the process network while considering all the stages in its life cycle from "cradle-to-gate." This is accomplished through mass and energy balances. To calculate the environmental burdens of the processes associated with the raw materials/utilities used in the industrial network, we use LCI data retrieved from environmental databases. This allows broadening the scope of the analysis to beyond the boundaries of the process network itself. In this work, we will assume that this information is uncertain. In mathematical terms, the LCI entry associated with environmental burden b (denoted by continuous variable LCI_b), is obtained from the net consumption of raw materials and utilities (inputs), along with the direct emissions and waste generated (outputs), as shown in Eq. 30

$$\begin{aligned}\mathrm{LCI}_b = &\sum_{k\in K}\left(\sum_{s\in \mathrm{SRMP}_k} M_s - \sum_{s\in \mathrm{SRMR}_k} M_s\right)\omega^{\mathrm{RM}}_{b,s}\,\mathrm{TOP}\\ &+\sum_{u\neq U2,U4}\mathrm{TCONS}_u\,\omega^{UT}_{b,u}+\sum_{s\in \mathrm{SDE}_b|b\in \mathrm{DE}} M_s X_{s,b}\mathrm{TOP}\\ &+\sum_{s\in \mathrm{SWA}_b|b\in \mathrm{WA}} M_s X_{s,b}\mathrm{TOP}\quad \forall b\in B\end{aligned} \tag{30}$$

where $\omega^{\mathrm{RM}}_{b,s}$ and $\omega^{\mathrm{UT}}_{b,u}$ are the LCI entries (i.e., emissions, waste generated, and feedstock requirements) per unit of raw material and utility, respectively, and TOP the total number of operating hours. As aforementioned, standard values of these parameters are available in environmental databases. Note that double counting is avoided in the calculations by subtracting the recycled raw materials from the total amount of raw materials consumed, as the impact of the former is already accounted for through other model equations. The symbols SDE_b and SWA_b appearing in Eq. 30 denote the set of direct emission streams and waste streams that lead to an environmental burden b, respectively. DE and WA are subsets of B representing direct emissions and waste materials, respectively. Finally $X_{s,b}$ denotes the fraction of b in stream s.

3. Phase 3: Impact Assessment

In this stage of the LCA, we translate the LCI into the corresponding environmental impact using a damage assessment model. The damage caused in impact category e (denoted by the continuous variable IMP_e) is determined as follows

$$\mathrm{IMP}_e = \sum_{b\in B}\mathrm{LCI}_b\,\theta_{b,e}\quad \forall e\in E \tag{31}$$

where $\theta_{b,e}$ is a damage factor that quantifies the impact per unit of direct emissions, waste, or feedstock requirement. By combining Eqs. 30 and 31, we get

$$\begin{aligned}\mathrm{IMP}_e = &\sum_{k\in K}\left(\sum_{s\in \mathrm{SRMP}_k} M_s\left(\sum_{b\in B}\omega^{\mathrm{RM}}_{b,s}\theta_{b,e}\right)\mathrm{TOP}\right.\\ &\left.-\sum_{s\in \mathrm{SRMR}_k} M_s\left(\sum_{b\in B}\omega^{\mathrm{RM}}_{b,s}\theta_{b,e}\right)\mathrm{TOP}\right)+\sum_{u\neq U2,U4}\mathrm{TCONS}_u\left(\sum_{b\in B}\omega^{\mathrm{UT}}_{b,u}\theta_{b,e}\right)\\ &+\sum_{b\in \mathrm{DE}}\sum_{s\in \mathrm{SDE}_b} M_s X_{s,b}\theta_{b,e}\mathrm{TOP}+\sum_{b\in \mathrm{WA}}\sum_{s\in \mathrm{SWA}_b} M_s X_{s,b}\theta_{b,e}\mathrm{TOP}\quad \forall e\in E\end{aligned} \tag{32}$$

which is a more convenient way to express Eq. 30, as environmental databases usually provide the value of the aggregated term $\sum_{b\in B}\omega_b\theta_{b,e}$. Hence, by replacing Eqs. 30 and 31 by Eq. 32, we avoid the explicit definition of variable LCI_b over B, a set that can contain in some cases hundreds of elements.

The total environmental impact, denoted by the continuous variable IMP, is determined from the impacts in each damage category as follows

$$\mathrm{ENVI} = g_{\mathrm{ENVI}}(\mathrm{IMP}_e) \tag{33}$$

where $g_{\mathrm{ENVI}}(\cdot)$ is a generic environmental function that can represent either a single LCA metric or an aggregated indicator.

4. Phase 4: Interpretation

In this phase, which is carried out in the post optimization analysis, the results are analyzed, and a set of conclusions and recommendations for the system are formulated.

Mathematical Formulation: Stochastic Model

We describe in this section how we obtain the stochastic model from the deterministic one. Hence, the stochastic model is constructed by slightly modifying the deterministic MINLP described before. More precisely, mass-balance constraints, utilities consumption constraints, and equations describing the performance of the process units remain unaffected. In contrast, the environmental constraints are modified to consider explicitly the uncertainty of the LCI data. Note that this source of uncertainty has no effect on the economic objective function.

Decision variables are classified as scenario independent and scenario-dependent. The former are insensitive to the materialization of the uncertain parameters, while the values of the latter depend on how the uncertainty is resolved. The variables used to model the LCI and LCIA results are the only scenario-dependent variables of the model. The sections that follow describe how the stochastic MINLP is constructed from its deterministic counterpart. Particularly, we provide details on the algebraic transformations that need to be made in the equations involved in the environmental impact calculations, which are the only ones modified.

Stochastic objective function

In the deterministic MINLP, the LCI is calculated from the flows of energy and mass associated with the main process. These are obtained from the consumption rates of utilities (i.e., electricity, steam, etc.) and raw materials, and the amount of direct emissions and waste generated (see Eq. 30).

Note that the LCI entries (i.e., parameters $\omega^{\mathrm{RM}}_{b,s}$ and $\omega^{\mathrm{UT}}_{b,u}$ in Eq. 30) enable us to enlarge the scope of the environmental analysis beyond the boundaries of the main process by translating the amounts of raw materials and utilities

consumed into the corresponding life-cycle environmental burdens. We now assume that these parameters, which are typically gathered from disperse sources, are uncertain. Equation 30 is, therefore, rewritten as follows

$$\tilde{\mathrm{LCI}}_b = \sum_{k\in K}\left(\sum_{s\in \mathrm{SRMP}_k} M_s - \sum_{s\in \mathrm{SRMR}_k} M_s\right)\tilde{\omega}^{\mathrm{RM}}_{b,s}\,\mathrm{TOP} + \sum_{u\neq U2,U4}\mathrm{TCONS}_u\,\tilde{\omega}^{\mathrm{UT}}_{b,u} + \sum_{s\in \mathrm{SDE}_b | b\in \mathrm{DE}} M_s X_{s,b}\,\mathrm{TOP} + \sum_{s\in \mathrm{SWA}_b | b\in \mathrm{WA}} M_s X_{s,b}\,\mathrm{TOP} \quad \forall b\in B \tag{34}$$

where $\tilde{\omega}^{\mathrm{RM}}_{b,s}$ and $\tilde{\omega}^{\mathrm{UT}}_{b,u}$ are stochastic parameters and $\tilde{\mathrm{LCI}}_b$ is a stochastic variable. Note that uncertainties in the LCI entries propagate to the impact assessment phase, thereby affecting the LCIA calculations. As a result, the damage in impact category e (denoted by continuous variable $\tilde{\mathrm{IMP}}_e$), which is determined from the LCI using a damage assessment model, must be regarded as stochastic

$$\tilde{\mathrm{IMP}}_e = \sum_{b\in B}\tilde{\mathrm{LCI}}_b\,\theta_{b,e} \quad \forall e\in E \tag{35}$$

Here, $\theta_{b,e}$ is the contribution of each LCI entry to the corresponding damage category. For simplicity, we consider herein nominal (i.e., deterministic) damage factors. Note, however, that our approach could be easily extended to handle uncertain damage factors. The total environmental impact, denoted by the stochastic continuous variable $\tilde{\mathrm{ENVI}}$, is determined from the impacts in each damage category as follows

$$\tilde{\mathrm{ENVI}} = g_{\mathrm{ENVI}}\left(\tilde{\mathrm{IMP}}_e\right) \tag{36}$$

where $g_{\mathrm{ENVI}}(\cdot)$ is a generic environmental function. As will be discussed in more detail later in the article, we focus herein on minimizing several single LCA-based indicators under uncertainty.

The overall multiobjective stochastic model can be finally expressed as follows

$$(\mathrm{PN})\ \min \mathrm{OF} = \{-\mathrm{ECOP}, \tilde{\mathrm{ENVI}}\}$$
$$s.t.\ \mathrm{Eqs.}\,1-29; 34-36$$

As observed, the economic objective function is the same as in the deterministic case, while the environmental impact is now regarded as stochastic. A key issue in this formulation is how to quantify and optimize the environmental impact in the uncertain parameter space. Standard stochastic optimization models attempt to identify robust solutions by optimizing the expected value of the objective distribution (see Sahinidis[22]). This strategy ensures the best average performance, but provides no control on its variability. As an example, consider an illustrative case with two process alternatives A and B. Figure 5 depicts the probability curves associated with them. A preliminary analysis would conclude that A (blue) is the preferred choice, as it shows better expected performance (median value 3.3) than B (red, median value 3.6). Closer inspection of the curves reveals that A implies a riskier attitude, as there is a (small) probability of higher environmental impact (i.e., above 4). More precisely, A has a 0.04 probability of exceeding a target environmental impact of 4, whereas this probability is zero in B. In other words, by selecting B, we make sure that the process will never surpass the environmental limit of 4, but this comes at the cost of a worst environmental performance on average.

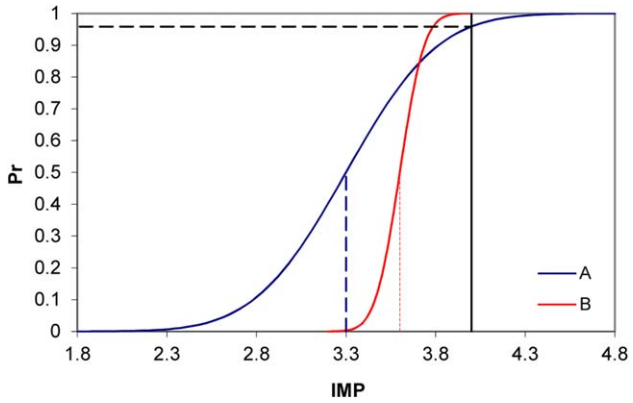

Figure 5. Probability curves associated with two generic solutions A (blue) and B (red).

[Color figure can be viewed in the online issue, which is available at wileyonlinelibrary.com.]

The goal of our analysis is to identify robust solutions with low probabilities of large impacts. As will be discussed later, this can be accomplished by optimizing stochastic metrics borrowed from financial risk management. Hence, rather than minimizing the expected value of the impact distribution (which is the standard approach in stochastic programming), we propose to minimize the probability of exceeding a given target value. This probability can be quantified by means of the following equation

$$\Pr\left\{\tilde{\mathrm{IMP}} \geq \Omega\right\} \leq \kappa \tag{37}$$

where we have omitted the subscript e indicating the specific impact category under study. The probability of violation of the uncertain inequality in Eq. 37 (i.e., the left-hand side representing the stochastic impact exceeds the right-hand side reflecting the desired target limit) is at most κ. Here, $\tilde{\mathrm{IMP}}$ denotes the "true" value of the impact, and κ represents the probability of violation of the constraint. A κ value of zero indicates that there is no chance of constraint violation, yielding the most conservative solution.

Equation 37 is a probabilistic or chance-constraint widely used in robust optimization (Ben-Tal and Nemirovski[39]). This constraint can be reformulated into a deterministic equivalent form, but only when the uncertain parameters follow specific types of uncorrelated probability functions.[40] This assumption seldom holds in LCA analysis. In our approach, we address this issue by discretizing the probabilistic constraints by means of scenarios. Equation 37 is, therefore, approximated via the following deterministic constraint

$$\Pr\left\{\tilde{\mathrm{IMP}} \geq \Omega\right\} = \sum_c \mathrm{prob}_c Z_c \quad \forall e \tag{38}$$

where prob_c is a parameter representing the probability of occurrence of scenario c, whereas Z_c is a binary variable that takes the value of 1 if the environmental impact exceeds the target limit in scenario c and 0 otherwise. The definition of this binary variable is enforced via the following constraints

$$\mathrm{IMP}_c \geq \Omega - M(1-Z_c) \quad \forall c$$
$$\mathrm{IMP}_c \leq \Omega + MZ_c \quad \forall c \tag{39}$$

where M is a sufficiently large parameter. The impact in scenario c is calculated from the LCI via the following constraint

$$\begin{aligned}\mathrm{IMP}_c = &\sum_{k\in K}\left(\sum_{s\in \mathrm{SRMP}_k} M_s\left(\sum_{b\in B}\omega^{\mathrm{RM}}_{b,s,c}\theta_b\right) - \sum_{s\in \mathrm{SRMR}_k} M_s\left(\sum_{b\in B}\omega^{\mathrm{RM}}_{b,s,c}\theta_b\right)\right)\\ &+\sum_{u\neq U2,U4}\mathrm{TCONS}_u\left(\sum_{b\in B}\omega^{\mathrm{UT}}_{b,u,c}\theta_b\right)+\sum_{b\in \mathrm{DE}}\sum_{s\in \mathrm{SDE}_b} M_s X_{s,b}\theta_b\\ &+\sum_{b\in WA}\sum_{s\in \mathrm{SWA}_b} M_s X_{s,b}\theta_b \quad \forall c\in C\end{aligned} \tag{40}$$

In this equation, $\omega^{\mathrm{RM}}_{b,s}$ and $\omega^{\mathrm{UT}}_{b,u}$ denote the values of the corresponding LCI entries in scenario c, which are generated from probability distributions using sampling techniques, while parameter θ_b is a damage factor that quantifies the contribution of the LCI entries to certain potential impacts defined in the goal and scope phase. Recall that, for simplicity in the derivation of the stochastic model, subscript e has been dropped from θ_b, $\omega^{\mathrm{RM}}_{b,s,c}$, $\omega^{\mathrm{UT}}_{b,u,c}$, and IMP_c.

The discretization of the probabilistic constraint requires definition of as many binary variables as scenarios. This leads to complex models with poor numerical performance (see Barbaro and Bagajewicz[41]). We propose to overcome this limitation by optimizing two stochastic metrics that are easier to calculate. In particular, we investigate the use of the downside risk[42] and the WC, both of which are widely applied in financial risk management, as a means to control the environmental impact under uncertainty. The downside risk (DRisk) is defined as the area enclosed above the cumulative probability curve between a target value and infinity. Mathematically, it is expressed as follows

$$\mathrm{DRisk} = \sum_c \mathrm{prob}_c\,\delta_c \tag{41}$$

where the definition of the auxiliary continuous variable δ_c (with the same unit as impact IMP) is enforced via the following constraints

$$\begin{aligned}&\delta_c \geq 0 \quad \forall c\\ &\delta_c \geq \mathrm{IMP}_c - \Omega \quad \forall c\end{aligned} \tag{42}$$

where variable IMP_c represents the impact attained in scenario c, and parameter Ω denotes a given target value that should not be exceeded. The WC is a risk metric that quantifies in our model the value of the largest impact that could materialize considering all the scenarios defined in the model. The value of this variable is determined according to the following equation

$$\mathrm{WC} \geq \mathrm{IMP}_c \quad \forall c \tag{43}$$

As observed, the downside risk penalizes the deviation from the target value, thereby accounting for both the probability of surpassing a given limit and the amount by which this target is exceeded. In contrast, the WC quantifies the environmental performance in the worst scenario (i.e., the scenario in which the emissions take the highest possible values). The downside risk and WC do not require binary variables. This simplifies to a large extent the mathematical formulation and leads to better numerical performance in the stochastic model.

Figure 6 shows the values of the three risk metrics (i.e., probability of not exceeding a target value, downside risk, and WC) for the illustrative example presented before. As

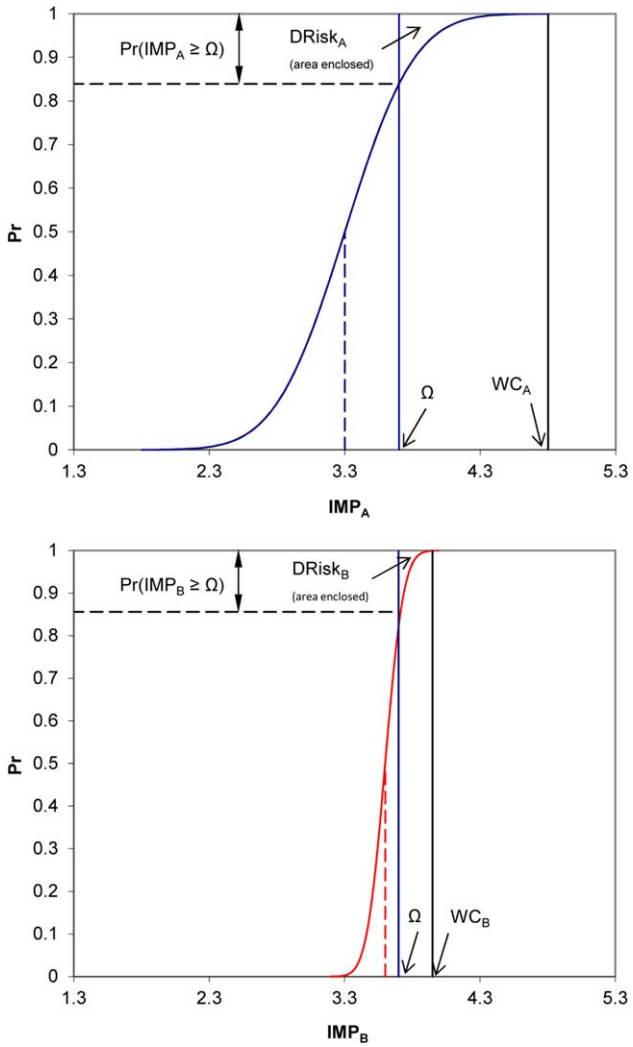

Figure 6. Probability of not exceeding a target value, downside risk, and WC for two generic solutions A (blue) and B (red).

[Color figure can be viewed in the online issue, which is available at wileyonlinelibrary.com.]

observed, the three metrics tend to behave similarly, that is, the minimization of one of them results typically in the minimization of the others.

We finally propose two MINLP formulations that differ in the stochastic metric minimized in the objective function

$$(\mathrm{MOPN\_DR})\ \min \mathrm{OF} = \{-\mathrm{ECOP}, \mathrm{DRisk}\}$$

$$s.t.\ \mathrm{Eqs.}1-29; 34-36; 40-42$$

For the case when the downside risk is optimized, and the following one when we use the WC

$$(\mathrm{MOPN\_WC})\ \min \mathrm{OF} = \{-\mathrm{ECOP}, \mathrm{WC}\}$$

$$s.t.\ \mathrm{Eqs.}1-29; 34-36; 40, 43$$

In the case study section, we will discuss the advantages and limitations of each model as applied to our particular problem.

Scenario generation: Building the probability functions

A critical issue in the multiscenario model is the generation of appropriate values of the uncertain parameters. In our

work, we obtain these values from probability functions by means of sampling techniques. The first step in our approach is, therefore, to obtain the probability functions of the uncertain parameters (i.e., LCI data) in an explicit form. These distributions can be constructed in three different manners. The first option is to retrieve them from environmental databases. Unfortunately, while most environmental databases provide the expected (nominal) values of the LCI parameters, very few contain probabilistic information. This lack of data hampers the stochastic modeling. The second alternative is to fit the distributions to historical data whenever this is possible. The third option is based on the approach proposed by Weidema and Wesnæs,[43] which uses qualitative information about the quality of the data available to build continuous distributions of the uncertain LCI parameters. The main advantage of this approach is that it can be readily applied even in those cases with very little information about the stochastic nature of the LCA data. We next provide a brief outline of this technique.

According to Weidema and Wesnæs,[43] the uncertain LCI parameters can be modeled using log-normal distributions [i.e., $\omega \sim \text{lnN}(\mu,\sigma)$, where we have dropped for simplicity the superscript and subscript of parameter ω]. Note that if a variable follows a log-normal (lnN from here on) distribution, then its natural logarithm is normally distributed. The lnN distribution is defined by two parameters: location parameter, μ and arithmetic scale parameter, σ. The arithmetic scale parameter is calculated from the geometric scale parameter (σ_g) as follows

$$\sigma=\ln(\sigma_g) \tag{44}$$

where the geometric scale parameter is estimated using Eq. 13

$$\sigma_g^2=\exp\left(\sqrt{(\ln U_1)^2+(\ln U_2)^2+(\ln U_3)^2+(\ln U_4)^2+(\ln U_5)^2+(\ln U_6)^2+(\ln UB)^2}\right) \tag{45}$$

Note that μ and σ are, respectively, the mean and standard deviation of the natural logarithm of the uncertain parameter, because by definition its logarithm is normally distributed. Factors U_1–U_6 appearing in Eq. 45 are obtained using the so-called Pedigree matrix[43] approach. This approach formulates a set of questions concerning the reliability (U1), completeness (U2), temporal correlation (U3), geographical correlation (U4), further technological correlation, (U5), and sample size (U6) of the LCI data. LCI data of poor quality lead to large U values (and, therefore, high uncertainty levels), whereas small U factors and low variability are obtained when high-quality data are available. Parameter UB is an uncertainty factor that depends only on the environmental burden. The mean value μ of the lnN distribution is calculated from the arithmetic scale parameter using the following constraint

$$\mu=\ln(E[\tilde{\omega}])-\frac{\sigma^2}{2} \tag{46}$$

where $E[\tilde{\omega}]$ denotes the expected (nominal/deterministic) value of the LCI entry, which is typically available in environmental databases. Hence, we assume that the LCI value retrieved from the environmental databases is the population arithmetic mean of the random variable. This "true" mean can be estimated by the expected value of a set of independent replications (i.e., scenarios). The same criterion holds for the standard deviation of the uncertain parameter. It should be clarified that for an infinite number of scenarios, the true mean and standard deviation of uncertain parameters should match the expected value and standard deviation of the samples (i.e., scenarios).

Once the distribution is fully defined, one can generate random values of the uncertain parameters (lying within the limits of the probability distribution) by means of sampling methods. This part is described in detail in the following section.

Scenario generation: Sampling methods applied to the multivariate probability functions

Representative scenarios of the uncertain parameter space are generated from the probability functions obtained in the previous step. A scenario is a sample of the n uncertain parameters (which are assumed to follow lnN distributions) that has a given probability of occurrence. The scenario generation procedure needs as input data the parameters of the uncertain distributions along with the correlation matrix describing the interactions between them.

Multivariate sampling methods accounting for correlated parameters typically assume that the uncertain data follow distributions other than the lnN (i.e., mainly normal distributions). To generate values for the lnN distribution from values that follow other distributions, we make use of a random number-generator coupled with the so-called inverse transform sampling method. The main theorem that supports this procedure states that if $F(x)$ is the cumulative distribution function (CDF) of random variable x, and the stochastic variable y follows a uniform distribution between 0 and 1, then the stochastic variable $z=F^{-1}(y)$ will follow the distribution of x. This theorem provides the mathematical foundation for generating values for any distribution for which we can compute its inverse. Hence, we generate the scenarios assuming that the uncertain parameters follow normal (Gaussian) distributions (N from here on), and then, recalculate these values making use of the transform sampling method. To generate scenarios for the N case, we need two parameters: the mean (μ_N) and the standard deviation (σ_N). These parameters are obtained as follows

$$\mu_N=E_N(\tilde{\omega}) \tag{47}$$

$$\sigma_N=\sqrt{\text{Var}_N(\tilde{\omega})} \tag{48}$$

where $E_N(\omega)$ denotes the expected value of the uncertain parameter, while $\text{Var}_N(\omega)$ corresponds to its variance. We assume that the expected value and variance of the N distribution are the same as those of the lnN distribution, that is

$$E_N(\tilde{\omega})=E(\tilde{\omega}) \tag{49}$$

$$\text{Var}_N(\tilde{\omega})=\text{Var}(\tilde{\omega}) \tag{50}$$

As aforementioned, the expected value $E_N(\tilde{\omega})$ of the lnN distribution can be retrieved from environmental databases, whereas the variance $\text{Var}_N(\tilde{\omega})$ is obtained from the (arithmetic) scale parameter of the lnN distribution as follows

$$\mathrm{Var}(\tilde{\omega}) = \exp(2\mu+\sigma^2)(\exp(\sigma^2)-1) \quad (51)$$

where the value of σ is calculated following the approach introduced by Weidema and Wesnæs[43] (Eqs. 44–46)

To account for correlations between emissions, we need to define the symmetric correlation matrix ρ that contains pairwise correlation information (i.e., 1 in the diagonal and numbers ranging between -1 and 1 in the remaining positions). If these numbers are close (or equal) to zero, then the variables are uncorrelated. Conversely, the variables are correlated when this value approaches either -1 (meaning that when one variable increases the other decreases linearly) or 1 (meaning that both variables increase and decrease linearly). To generate the required number of scenarios, we, therefore, need the parameters of the N distributions and the correlation factors. We first apply a standard multivariate sampling algorithm to generate values of the uncertain parameters for the N case. The inverse transform sampling is then applied to translate these values to the lnN case. This is done in two steps. Let ω_c be the value of the random parameter $\tilde{\omega}$ in scenario c. The normal cumulative distribution function (CDF) is first applied to ω_c to obtain a uniform distribution in the [0,1] interval (recall that we know the mean and standard deviation of the underlying Gaussian distribution, so the CDF can be readily computed). We then calculate the lnN inverse cumulative distribution function of the values (distributed within the [0,1] interval), generating new values of ω_c that follow the correlated lnN distributions sought.

Scenario generation: Minimum number of scenarios

Another critical issue in the multiscenario MINLP is the minimum number of scenarios (i.e., samples) required to ensure that the stochastic metrics calculated with discrete samples are good estimators of their "true" values in the universe of uncertain parameters. For simplicity, we apply the method proposed by Law and Kelton,[44] which is valid for stochastic programming models that optimize the expected value of the objective function distribution. This approach relies on solving the stochastic model that maximizes the expected value of the impact distribution for an increasing number of scenarios. The goal is to obtain an estimate of the mean of the "true" objective function distribution (considering the entire set of uncertain parameters) with a given relative error γ and confidence level $100(1-\alpha)\%$. In the context of our problem, this method comprises the following steps:

1. Define an initial number of scenarios ns_0, and make $|C| = ns = ns_0$, where ns will be updated dynamically during the execution of the algorithm.

2. Solve the following stochastic model that maximizes the expected impact with $|C| = ns$ scenarios

$$\min \mathrm{OF} = \sum_c \mathrm{prob}_c \mathrm{IMP}_c$$

$$s.t. \ \mathrm{Eqs.}1-29;40$$

3. Compute the confidence-interval half-length $\delta(ns,\alpha)$ for the mean impact from the values of the impact in each scenario (IMP_c) as follows

$$\delta(ns,\alpha) = t_{n-1,\frac{1-\alpha}{2}} \sqrt{\frac{\mathrm{Var}^2(ns)}{ns}} \quad (52)$$

where $\mathrm{Var}^2(ns)$ is the sample variance of the impact distribution, and $t_{n-1,\frac{1-\alpha}{2}}$ is the critical point of the t-distribution.

4. If $\frac{\delta(ns,\alpha)}{|E[\mathrm{IMP}]|} \leq \frac{\gamma}{1-\gamma}$, then stop (i.e., the expected value of the discrete distribution is a valid estimator of the mean of the universe for the relative error and confidence interval defined beforehand). Otherwise, make $ns = ns + 1$ and go to Step 2.

More details about this procedure can be found in the work by Law and Kelton.[44]

Solution Procedure

Several MOO algorithms can be used for solving the multiobjective models described above. Without loss of generality, we use here the epsilon constraint method,[45] which is based on calculating a set of single-objective problems in which all objectives but one are transferred to auxiliary constraints that impose bounds on them. Details on this solution method can be found elsewhere.[46]

Note that each iteration of the epsilon constraint algorithm entails the solution of a large-scale nonconvex MINLP. Several MINLP algorithms can be used in the calculations, such as the outer-approximation (implemented in DICOPT), extended cutting plane (AlphaECP), and nonlinear branch and bound (SBB) methods (see the review article on MINLP by Grossmann[47] for further details).

The MINLP model shows many distinct types of nonconvexities. Bilinear terms appear in the mixers equations, while process correlations include multilinear, exponential, and fractional terms of different forms. These nonconvexities give rise to multiple local optima (i.e., multimodality) at which local solvers could fail during the search. Furthermore, even finding a feasible starting point (i.e., initial guess) for the optimization algorithm is a hard task. Rigorous deterministic global optimization methods, which are the only ones that guarantee convergence to the global optimum, lead to prohibitive computational times because of the size and complexity of the model. To overcome this difficulty, we used multiple starting points in the calculations in an attempt to identify the global optimum. To define these initial guesses, we devised a customized initialization scheme based on solving the units sequentially. The strategy works as follows. The operating conditions of the first unit along with the properties and flow rates of its input streams are initialized. The equations of this unit are then solved, providing the properties and flow rates of the output streams. These values are used in the equations of those units located immediately after the first. This procedure is repeated sequentially until the storage tanks are reached. Split ratios and utilities consumption rates are initialized based on prior knowledge of the system. Each run of the initialization scheme provides a different point that is used in the execution of the MINLP solver. The local optimizer is, therefore, executed from the starting points obtained through this procedure in an attempt to identify the global optimum. Note, however, that the solutions obtained with this method must be regarded only as locally optimal.

Remarks

The following key aspects of our approach are highlighted next before presenting some numerical results:

- When the uncertain parameters are modeled with discrete distributions, there is no need to perform any sampling. In this case, we can incorporate the discrete distribution explicitly in the MINLP formulation.

- Our approach can handle any type of probability distribution and can also deal with correlations between uncertain parameters.
- The deterministic MINLP that minimizes the impact in the most likely (i.e., mean) scenario produces the same result as the stochastic MINLP that minimizes the expected impact for a sufficiently large number of scenarios.

Case Study

We illustrate the capabilities of our modeling framework and solution strategy using the process network introduced previously. We describe first some results obtained with the deterministic model that shed light on the inherent trade-offs between the economic and environmental performance of the industrial network. We then use the stochastic formulation to address the uncertainty pertaining to the main feedstock of the process.

Deterministic case

We consider first two deterministic case studies that differ in the cost data used. For each, we solve three bicriteria problems where the economic performance is traded-off against the environmental impact, which is evaluated via three different LCA-based metrics: Metric 1, Metric 2, and Metric 3.

Quality specifications are defined for properties A–F in final products P1–P4. We assume a minimum demand satisfaction level of 100%, that is, the final products demand must be fully covered. Two sets of cost data are considered: Year I and Year II prices. The impacts per unit of raw material and utility generated were retrieved from Ecoinvent.[48] We consider seven direct emissions: DE:= {C1,...,C7}. Compounds C1, C2, and C3 contribute to Metric 1, C4 and C5 to Metric 2, and C4, C5, C6, and C7 to Metric 3. The goal of the analysis is to determine the optimal operating conditions and stream flows, as well as the type of fuel used in each process unit that simultaneously optimize economic performance and environmental impact.

The problem described above leads to a moMINLP model with 56 binary variables, 2144 continuous variables and 2405 constraints that is implemented in GAMS.[49] In this MINLP, binary variables are used to model the selection of a specific fuel type in each process unit. The single-objective MINLPs used in the epsilon constraint method are solved with the SBB solver on an AMD Phenom ^{TM} 8600 B Triple-Core 2.3 GHz Windows machine with 2048 MB of memory. The CPU time spent in each single-objective MINLP varies depending on the instance being solved, but is always less than 1 min. A detailed discussion of the deterministic results follows.

Economic dataset of Year I

In this numerical case, we consider prices, where, on an energy basis, U1 is slightly cheaper than U3. In addition, the selling prices for final products P1, P2, P3, and P4 expressed on a volume basis are much higher than those corresponding to byproducts P5, P6, and P7.

We first optimized economic performance and Metric 1. The maximum economic performance solution shows an economic performance of 175 economic units/yr and an environmental impact of 2.93 units of Metric 1/yr. In contrast, the economic performance of the minimum environmental impact solution is 134 economic units/yr while the environmental impact is 2.64 units of Metric 1/yr. These two optimizations provided the upper and lower bounds for the epsilon parameters. Following the standard epsilon constraint method, we partition this interval into subintervals of equal length and solved a set of single-objective MINLPs in which we maximize economic performance and force the environmental impact to be lower than the limits of each of these subintervals. The Pareto set of solutions obtained through this procedure is depicted in Figure 7. As observed, there is a clear trade-off between the economic and environmental performance of the process network as an improvement in one can only be achieved at the expense of compromising the other.

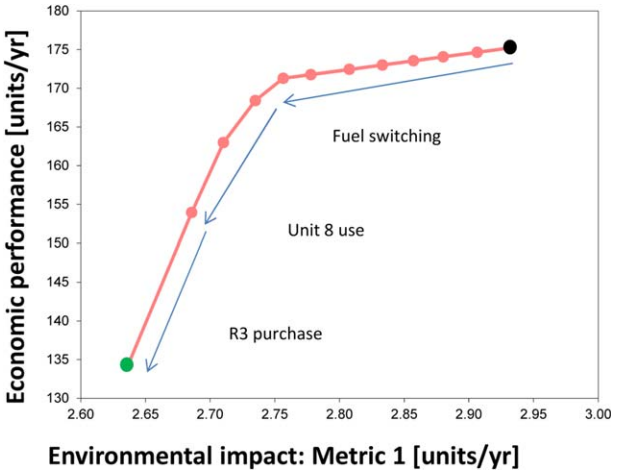

Figure 7. Set of Pareto optimal solutions that trade-off economic performance vs. environmental Metric 1 at Year I prices.

[Color figure can be viewed in the online issue, which is available at wileyonlinelibrary.com.]

Figures 8 and 9 depict the process network configurations associated with the extreme solutions. As seen, in the maximum economic performance solution, Units 1, 5, and 9 operate with fuel U1, Units 4 and 7 use fuel U4, and Unit 6 a mix of fuel U3 (purchased externally) and U4 (recycled internally). In contrast, in the minimum environmental impact solution, Units 4, 5, and 9 consume a mix of fuel U3 and U4, whereas Units 1, 6, and 7 consume only fuel U3, and Unit 8 only fuel U4. The solutions differ mainly in the switch from fuel U1 to U3, and in the use of Unit 8, which is operated in the minimum environmental impact case alternative but is bypassed in the maximum economic performance configuration. R3 is purchased in the minimum environmental impact alternative, but its consumption is zero when maximizing economic performance. Both configurations avoid the use of Units 2 and 3. The two extreme solutions also lead to different flow rates and operating conditions that are not discussed here due to space limitations.

Intermediate solutions in between the extreme alternatives are represented by circles in Figure 7. The first seven intermediate solutions starting from the right-hand side of the Pareto set reduce the environmental impact by progressively replacing fuel U1 by U3/U4 in the process units. A point in the curve is then reached as we move to the left in which fuel switching is unable to reduce the environmental impact any further. The model then chooses to start operating Unit

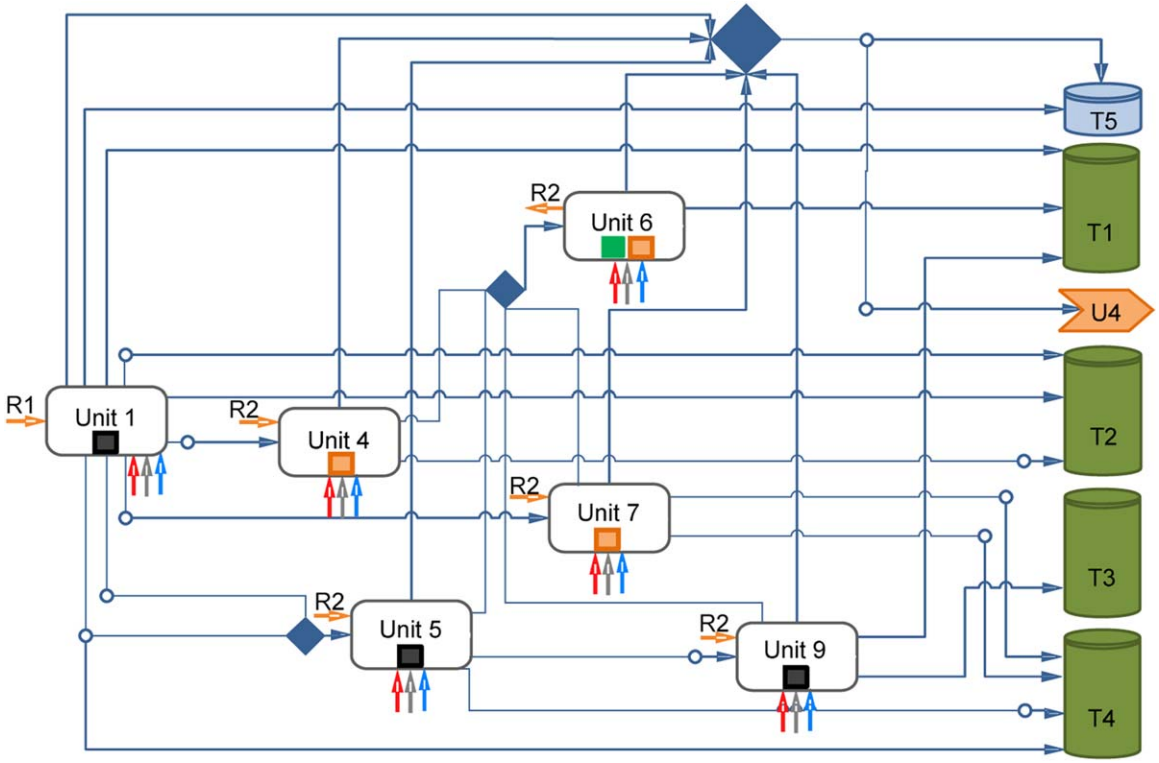

Figure 8. Optimal process configuration for the maximum economic performance solution with Year I data.

Units 2, 3, and 8 are inactive. Fuel U1 is used to power Units 1, 5, and 9, whereas fuel U4 is used in Units 4 and 7. Unit 6 works with a mix of fuels U3 and U4. Raw materials R1 and R2 are purchased externally, while raw materials R3 and R4 are not consumed. [Color figure can be viewed in the online issue, which is available at wileyonlinelibrary.com.]

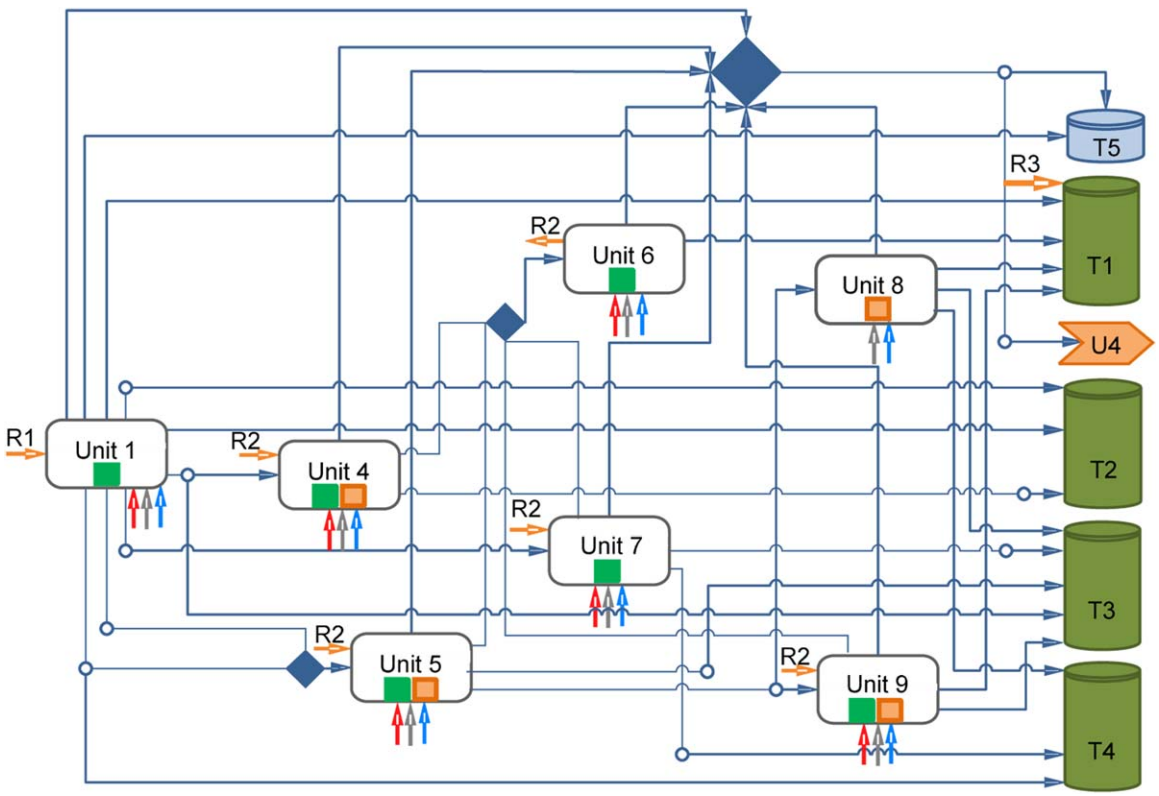

Figure 9. Optimal process configuration for minimum environmental impact (Metric 1) solution with Year I data.

Units 2 and 3 remain inactive, while Unit 8 is activated. Fuel U1 is avoided. Units 4, 5, and 9 use a mix of fuels U3 and U4, Units 1, 6, and 7 work with fuel U3, and Unit 8 makes use of fuel U4. Raw material R3 is now purchased along with raw materials R1 and R2, while R4 is not consumed. [Color figure can be viewed in the online issue, which is available at wileyonlinelibrary.com.]

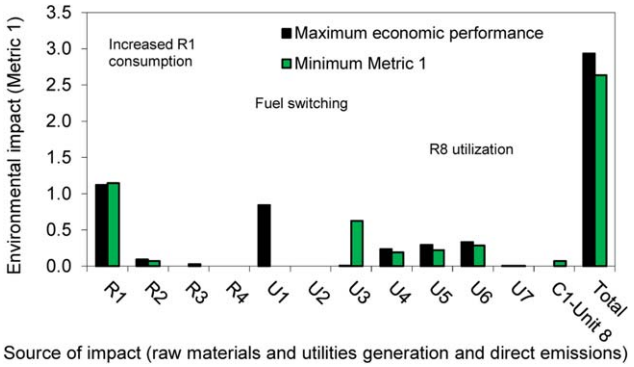

Figure 10. Breakdown of sources of environmental impact contributing to Metric 1 at Year I prices.

[Color figure can be viewed in the online issue, which is available at wileyonlinelibrary.com.]

8 and redistribute the internal flows within the process network. This change in the values of the flow rates has the effect of increasing the consumption of raw material R1 while decreasing at the same time the input flow rates to some of the process units. This nonintuitive strategy is analyzed in greater detail with the help of Figure 10. The environmental savings associated with decreasing the input flow rates to some of the process units, and hence, the utilities consumed by them, offsets the increase in the consumption of raw material R1 in a manner that the total impact as measured by Metric 1 is reduced. The two points located leftmost in the Pareto set implement a third strategy to reduce environmental impact, which consists of purchasing raw material R3 from an external supplier. The motivation for this is that, according to the environmental data available in Ecoinvent,[48] producing R3 externally causes less life cycle impact than generating it internally (but leads, at the same time, to higher costs).

Figure 10 shows a breakdown of the main sources of environmental impact contributing to Metric 1 for the extreme solutions of the Pareto set. The figure displays on the horizontal axis the main contributors to Metric 1, including the generation of raw materials R1–R4, utilities U1–U7, and the direct emissions of compound C1 by Unit 8. The vertical axis is the impact (quantified via Metric 1) due to each source. The last two bars depict the total environmental impact (expressed in Metric 1 units per year) for the extreme solutions. The impact of the recycled fuels U2 and U4 is due only to the direct emissions from their combustion. In contrast, the impact associated with fuels U1 and U3 accounts for the environmental burdens occurring during both production and combustion.

In the maximum economic performance solution, the main source of impact is the generation of R1, followed by the production of U1, U6, U5, U4, and R2. In contrast, in the minimum environmental impact solution, the sources of impact are ranked as follows (in a descending order): R1, U3, U6, U5, U4, C1, R2, and R3. The impacts associated with R4 and U2 are zero in both cases as these materials are not consumed in either extreme configuration. In addition, the impact of U7 is very small in the two solutions. Furthermore, the impact of U1 takes a high value in the maximum economic performance solution and zero in the minimum impact case. In contrast, the bar associated with U3 is large in the minimum impact alternative and almost zero in the other extreme solution. Recall that U1 is replaced by U3 to reduce environmental impact, which comes at the expense of economic performance. Notice also that the bar corresponding to C1, a compound released by Unit 8, takes a zero value in the maximum economic performance solution, in which Unit 8 is inactive, and a small positive value in the minimum impact case in which the unit is used. Similarly, the contribution of raw material R3 to the total impact is zero in the maximum economic performance solution, as this raw material is not purchased.

As seen in the figure, the minimum impact solution increases the consumption of raw material R1 by implementing a fuel balancing strategy. Further analysis of the extreme solutions reveals that the environmental savings achieved by reducing the consumption of U4, U5, U6, and R2 via flow balancing offset the negative impact of increasing the amount of R1 required. This is the kind of nonintuitive solution that mathematical programming can generate, and would be difficult to identify using conventional approaches like rules of thumb or heuristics.

Next, we solved two additional bicriteria problems considering two additional environmental metrics: Metric 2 and 3. Figure 11 shows the Pareto sets of the three bicriteria problems (i.e., economic performance vs. Metric 1, 2, and 3, respectively). The horizontal axis displays the normalized environmental indicator, and the vertical axis shows the normalized economic performance. The normalization is performed by dividing each value by its corresponding maximum value over all points of each set. As observed, the largest reduction in environmental impact corresponds to Metric 3, followed by Metric 2 and Metric 1. Note that in all of the cases, the Pareto curve is flatter in the region close to the maximum economic performance configuration, but there is a bigger drop in the economic performance as we move toward the minimum impact solution.

The effect of considering a flexible demand, that is, of allowing the model to exceed the demand was also

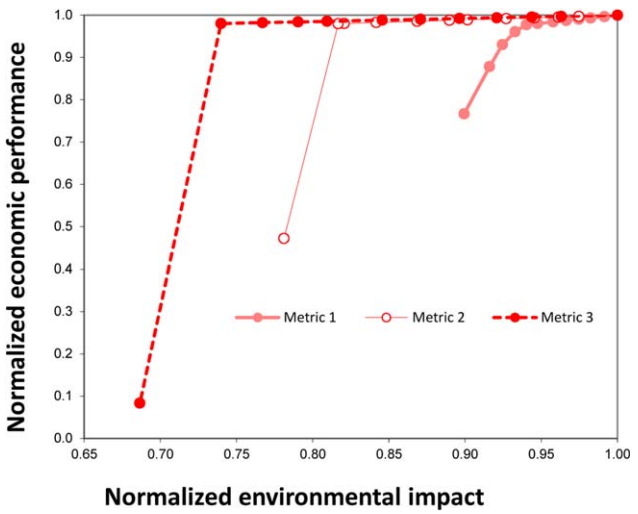

Figure 11. Set of Pareto solutions comparing economic performance against each environmental impact metric (i.e., Metric 1, Metric 2, and Metric 3) separately with Year I data.

[Color figure can be viewed in the online issue, which is available at wileyonlinelibrary.com.]

Table 1. Comparison of Flexible Supply Against Fixed Supply

Process Components Analyzed	Maximizing Economic Performance (Flexible Supply Value/Fixed Supply Value)	Minimizing Environmental Metric 1 (Flexible Supply Value/Fixed Supply Value)
P1 supply	1.08	1.00
P2 supply	1.10	1.00
P3 supply	1.10	1.00
P4 supply	1.00	1.10
P5 supply	1.07	1.04
Energy from U1	1.09	–
Energy from U3 + U4	1.08	0.97
Economic performance	1.18	0.82
Metric 1	1.08	0.99
Metric 2	1.08	1.02
Metric 3	1.08	1.02

investigated. For this purpose, we recalculated the extreme solutions, but this time allowed the model to surpass the demand by no more than 10%. The results obtained are displayed in Table 1.

Table 1 is composed of three columns. The first shows the products that are supplied, energy usage associated with U1 and U3/U4, and economic performance and environmental impact metrics. The second column shows the ratio between the values of these variables in the flexible and fixed demand cases for the maximum economic performance scenario, while the third column provides the same information for the case when Metric 1 is minimized.

As is evident, economic performance is increased by 18% when a flexible demand scenario is considered. The environmental impact metrics increase as well, by 8%. In contrast, minimizing Metric 1 under a flexible demand reduces economic performance by 18%, but lowers only 1% the value of Metric 1, and worsens by 2% Metrics 2 and 3. These results suggest that the model has the flexibility to vary economic performance but is rather rigid from the standpoint of decreasing environmental impact. In other words, it is easier to increase the economic performance when flexible demands are considered than to decrease the environmental impacts. Another interesting observation is that reducing Metric 1 does not necessarily imply that Metrics 2 and 3 will also be reduced.

With regard to the solutions resulting from the flexible demand cases, no structural changes are implemented when maximizing economic performance vs. the fixed demand case. In contrast, the minimization of Metric 1 with a flexible demand leads to some changes that deserve further discussion. The input flow rate to Unit 8 is increased, which allows the model to reduce the impact by 1%. Furthermore, this solution does not purchase intermediate products R3 and R4. This new alternative increases the production rates of P4 and P5, and at the same time reduces the overall energy consumption by 3% as observed in Table 1. This is a nonintuitive approach to reduce the impact, one that would have been hard to identify without the aid of systematic tools.

Table 2. Product Quality Specifications for the Maximum Economic Performance Case (NL Means that the Constraint is not Limiting, "Limits" Indicates An Active Constraint and a 'dash' Refers to Properties Which are not Defined for the Associated Products)

	Property					
Product	A	B	C	D	E	F
P1	NL	NL	Limits	NL	–	–
P2	NL	NL	–	–	NL	–
P3	NL	NL	–	–	–	NL
P4	NL	NL	–	–	–	–

Table 3. Product Quality Specifications for the Minimum Metric 1 Solution (NL Means That The Constraint is not Limiting, "Limits" Indicates An Active Constraint and a 'dash' Refers To Properties Which are not Defined for the Associated Products)

	Property					
Product	A	B	C	D	E	F
P1	NL	NL	Limits	NL	–	–
P2	NL	NL	–	–	NL	–
P3	NL	NL	–	–	–	NL
P4	Limits	NL	–	–	–	–

A sensitivity analysis was performed to identify the most critical constraints, that is, those with the strongest influence on the outcome of the model. Tables 2 and 3 show the results of this analysis. Here, product qualities that are not at their limiting value are labeled as NL. Note that the inequality constraints enforcing specifications of type NL are inactive at the optimal solution (i.e., they are satisfied as "strictly lower than" and not as equalities as their Lagrangian multipliers are zero). Conversely, "Limits" in Table 2 means that the quality specification has reached its limit (i.e., the inequality is satisfied as equality, and the Lagrangian multiplier is positive, thereby making the constraint active). A "dash" in the table indicates that the property is not defined for that product.

As observed in both cases (maximum economic performance and minimum environmental impact) property C of product P1 is limiting. To further investigate the effect of this quality specification, we performed a sensitivity analysis in which the bound imposed on this property was varied by 5% (see Table 4). We assume that the flexibility in the value of property C does not have any impact on the product price. As seen, when we relax this constraint by 5% (i.e., we allow a quality level 5% below the desired target value), we observe a very small variation in the objective function. In contrast, when the quality limit is 5% more strict, the economic performance drops by 30%. This analysis, therefore, reveals that the model is very sensitive in economic terms to increments in the quality specification imposed on property C of product P1.

Table 4. Sensitivity Analysis On Quality Specification C Defined for P1 for the Maximum Economic Performance Solution

		Maximizing Economic Performance	
Product	Constraint Modification	Normalized Economic Performance	Normalized Environmental Metric 1
P1	Property C − 5%	1.01	0.99
	Property C + 5%	0.70	1.04

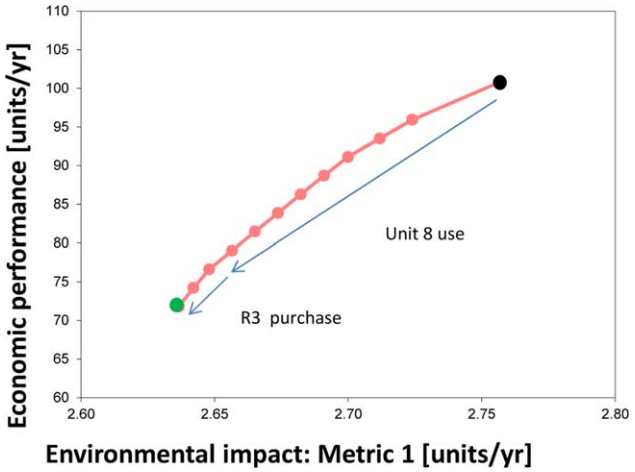

Figure 12. Set of Pareto optimal solutions that trade-off economic performance vs. environmental Metric 1 at Year II prices.

[Color figure can be viewed in the online issue, which is available at wileyonlinelibrary.com.]

The reader should note that the outcome of the analysis performed herein may vary according to the economic and environmental data considered in the optimization. Our systematic approach, however, provides valuable insights for each scenario being investigated, guiding decision-makers toward the adoption of manufacturing patterns that lead to improved economic and environmental performance.

Economic dataset of Year II

In this second case, we consider prices in Year II, where fuel U1 is about twice as expensive as U3 on an energy basis, while the prices of final products, raw materials, and utilities are all lower than in Year I.

Following the same procedure as before, we first solved the bicriteria problem that optimizes the economic performance and Metric 1. In Figure 12, the Pareto front corresponding to Year II prices is depicted using the same coloring scheme as Figure 7. The black point represents the maximum economic performance solution, whose process flow sheet configuration is presented in Figure 13, while the green point corresponds to the minimum impact alternative (see Figure 14). The economic performance is reduced from 101 economic units/yr to 72 economic units/yr to decrease the environmental impact from 2.76 units of Metric 1/yr to 2.64 units of Metric 1/yr. Again, there is a clear trade-off between the economic and environmental performance of the process network as an improvement in one can only be achieved at the expense of the other.

As seen in Figure 13, in the design corresponding to the maximum economic performance, Units 4 and 7 are run using internally recycled fuel U4, while units 1, 6, and 9 operate with fuel U3 (which is externally purchased). Unit 5 is powered by a combination of both fuels. Recall that the maximum economic performance solution for Year I prices selected fuel U1 in certain process units (i.e., Units 1, 5, and 9), which is avoided in this new case. In both cases (Years I and II prices), Units 2, 3, and 8 are inactive.

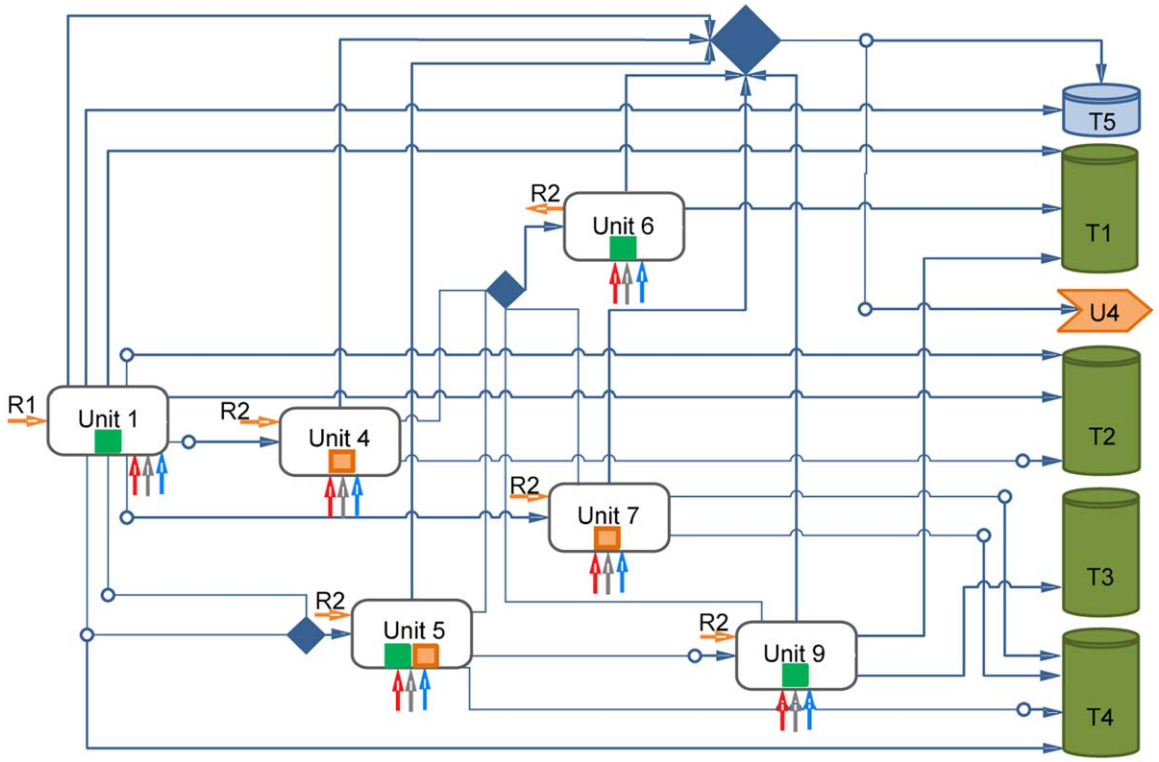

Figure 13. Optimal process configuration for the maximum economic performance solution with Year II data.

Units 2, 3, and 8 are inactive. Fuel U3 is used to power Units 1, 6, and 9, while Units 4 and 7 work only with fuel U4. Unit 5 works with a mix of fuels U3 and U4. Raw materials R1 and R2 are purchased externally, while raw materials R3 and R4 are not consumed. [Color figure can be viewed in the online issue, which is available at wileyonlinelibrary.com.]

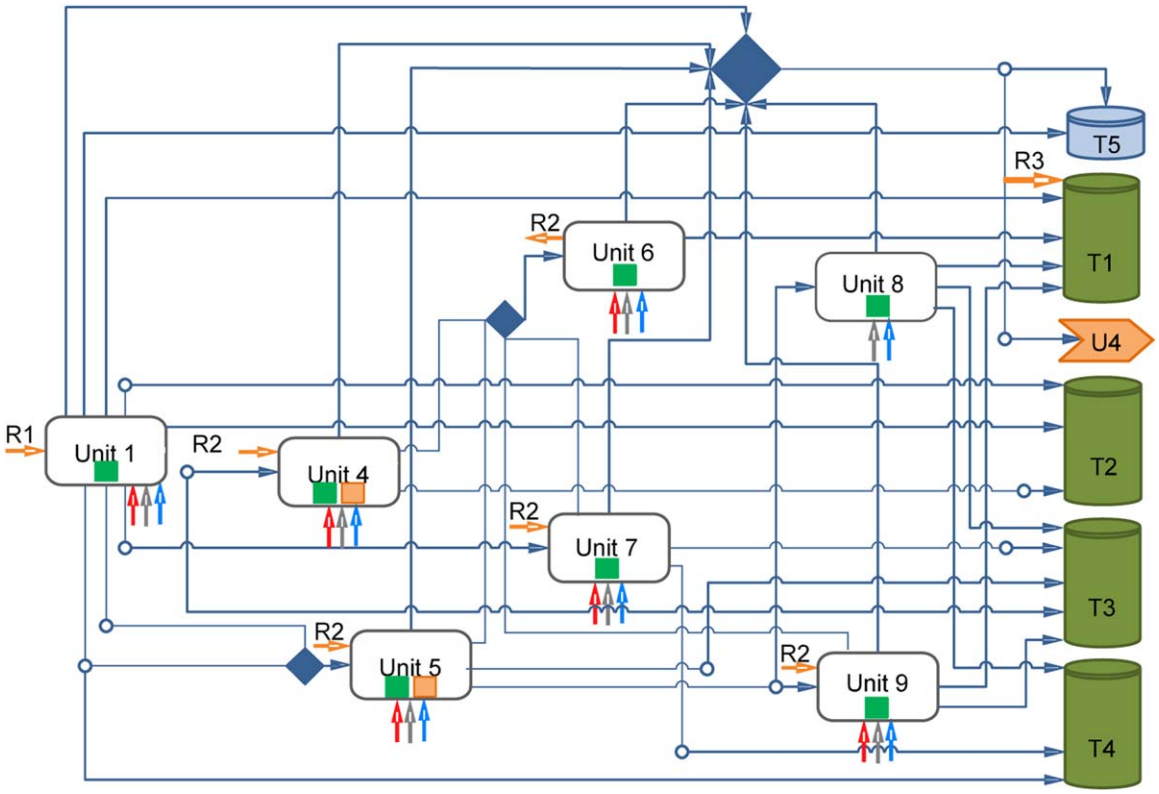

Figure 14. Optimal process configuration for the minimum environmental impact (defined by Metric 1) solution with Year II data.

Units 2 and 3 remain inactive, while Unit 8 is activated. Fuel U1 is avoided. Units 4 and 5 use a mix of fuels U3 and U4, while Units 1, 6, 7, 8, and 9 operate with fuel U3. Raw material R3 is now purchased along with raw materials R1 and R2, while R4 is not consumed. [Color figure can be viewed in the online issue, which is available at wileyonlinelibrary.com.]

In the minimum impact solution (see Figure 14), Units 1, 6, 7, 8, and 9 operate with fuel U3, while Units 4 and 5 are run with a mix of U3 and U4.

As we move from the maximum economic performance to the minimum environmental impact solution, the model first increases the input flow rate to Unit 8 gradually to reduce the environmental impact. This strategy increases the amount of raw material R1 that has to be processed, reducing at the same time the consumption rates of U3, U4, and U5 (and thereby the impact caused during their generation). Hence, operating Unit 8 is appealing from an environmental standpoint, but worsens the economic performance. When the model is unable to reduce the environmental impact any further by making use of Unit 8, it starts purchasing intermediate product R3 (note that this strategy is implemented in the last three points of the Pareto front). This is because in this case producing R3 externally entails a lower impact than generating it internally.

As done in the previous case, we solved two more bicriteria problems considering two additional environmental metrics: Metric 2 and 3. The results are depicted in Figure 15. The horizontal axis displays the normalized environmental indicator, and the vertical axis shows the normalized economic performance. The normalization was performed by dividing each value by the maximum over all the points of each set. There is a significant drop in the economic performance of the industrial network on trying to reduce the three different environmental impact metrics.

Stochastic analysis for Year I prices

We solve the first case study (considering cost data of Year I) but this time taking into account the uncertainty

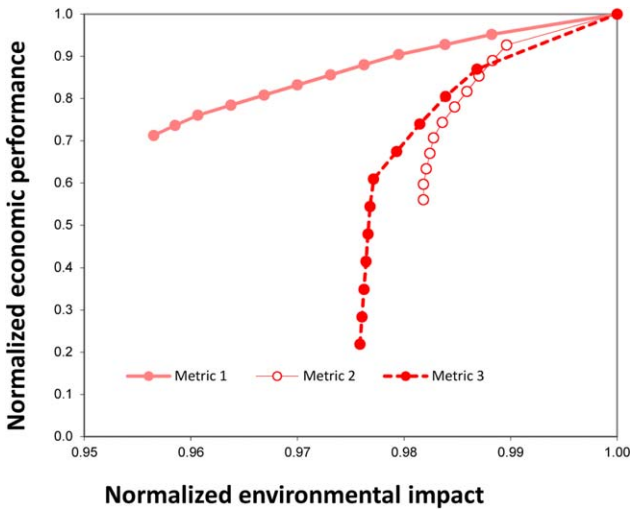

Figure 15. Set of Pareto solutions showing the trade-off between the economic performance and each environmental metric (i.e., Metric 1, Metric 2, and Metric 3) separately at Year II data.

[Color figure can be viewed in the online issue, which is available at wileyonlinelibrary.com.]

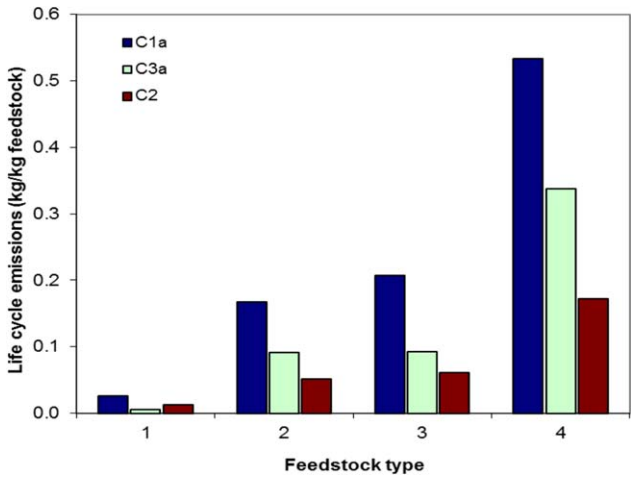

Figure 16. Life-cycle emissions of feedstocks similar to R1 (data from Ecoinvent[48]).

[Color figure can be viewed in the online issue, which is available at wileyonlinelibrary.com.]

associated with the life-cycle emissions of the main feedstock (i.e., R1 in Figure 1), which is one of the major sources of impact. For simplicity, we address the optimization of one single LCA-based indicator (Metric I) in the face of the aforementioned source of uncertainty. We restrict our analysis to only three of the 65 emissions that contribute to Metric 1 (i.e., compounds C1–C3) that are responsible for 99% of the total impact in the maximum economic performance solution. The nominal life-cycle emissions associated with the generation of the main feedstock (i.e., emissions released in the production of R1) were retrieved from Ecoinvent.[48] Compound C1 is present in two forms C1a and C1b, and Compound C3 is also found in two distinct forms C3a and C3b.

The first step before performing the calculations was to generate the scenarios used in the MINLP. To this end, we first need to obtain the distributions of the uncertain parameters (i.e., life-cycle emissions associated with the production of R1). In our case study, we assume that these parameters follow lnN distributions. The geometric standard deviation was estimated using the approach introduced by Weidema and Wesnaes,[43] which translates specific information on the quality of the data available into quantitative one (i.e., geometric scale parameter of the lnN distribution). Conversely, the expected (nominal) emissions were retrieved from Ecoinvent.[48] Hence, we assume that the database provides the nominal impact (i.e., expected impact). Realistic correlation coefficients were determined based on an analysis of the life-cycle emissions associated with similar feedstocks. Figure 16 compares the life-cycle emissions of our main feedstock R1 with those corresponding to three similar feedstocks.

Table 5. Pearson's Correlation Coefficient Between Compounds

	C1a	C2	C3a
C1a	1	0.9983	0.9948
C2	0.9983	1	0.9984
C3a	0.9948	0.9984	1

As seen, emissions C1a, C2, and C3a are correlated, as they all behave similarly. To confirm this, we next calculated the Pearson's correlation coefficient ρ, a well-known measure of the linear relationship between variables. This coefficient ranges from -1 (when one variable linearly decreases as the other increases) to 1 (when both variables increase and decrease linearly). A Pearson's coefficient of 0 implies no linear dependence. As observed, this coefficient was above 0.99 for the three compounds (see Table 5), indicating high correlation between them.

After this first preliminary analysis, we defined three case studies that differed in the uncertainty factors and degree of correlation considered. Our aim was to study the effect that the level of uncertainty and correlation between parameters have on the outcome of the optimization. We, therefore, defined the following cases.

Cases 1, 2, and 3 consider "realistic" scores of the factors of the Pedigree matrix (see Table 6), which were fixed according to the quality of the information available. The basic uncertainty factor UB was retrieved from the Ecoinvent report 1 (Overview and Methodology),[48] while the remaining parameters were obtained by answering the questions of the Pedigree matrix. These three case studies differ in the degree of correlation considered between emissions. In particular, Case 1 assumes no correlation (i.e., uncorrelated case: $\rho_{ij} = 0$ for all i,j with $i \neq j$). In contrast, Case 2 considers a correlation coefficient of 0.9 between C1a and C3a ($\rho_{C1aC3a} = \rho_{C3aC1a} = 0.9$), while in Case 3 the correlation coefficient is 0.9 for pairs C1a–C2, C1a–C3a, and C2–C3a: ($\rho_{ij} = 0.9$ for $i,j =$ C1a, C2, C3a with $i \neq j$). We will refer to the latter case as the fully correlated case.

The MINLPs were implemented in GAMS 23.3.3 and solved using an AMD Phenom ^{TM} 8600 B Triple-Core 2300 MHz processor machine with SBB as MINLP solver, and CONOPT 3.0 as NLP subproblem solver. The computational time required for solving each MINLP varied from 10 to 40 s depending on the instance being solved. We determined the minimum number of scenarios for the case with the most severe degree of uncertainty and correlation (i.e., Case 3). For a relative error of 0.1 and a confidence level of 0.7%, the minimum number of scenarios obtained using the procedure proposed by Law and Kelton[44] is 100. A discussion of the numerical results follows.

Economic Dataset of Year I: Case Studies 1 to 3. To illustrate the limitations of neglecting uncertainties, we

Table 6. Scores Given in the Pedigree Matrix to Each Criteria and Substance in Cases 1, 2 and 3

Compound	Reliability (U_1)	Completeness (U_2)	Temporal Correlation (U_3)	Geographical Correlation (U_4)	Further Technological Correlation (U_5)	Sample Size (U_6)	UB
C1a	1.1	1.2	1.0	1.1	1.2	1.2	1.05
C1b	1.1	1.2	1.0	1.1	1.2	1.2	1.05
C2	1.1	1.2	1.0	1.1	1.2	1.2	1.5
C3a	1.1	1.2	1.0	1.1	1.2	1.2	1.5
C3b	1.1	1.2	1.0	1.1	1.2	1.2	1.2

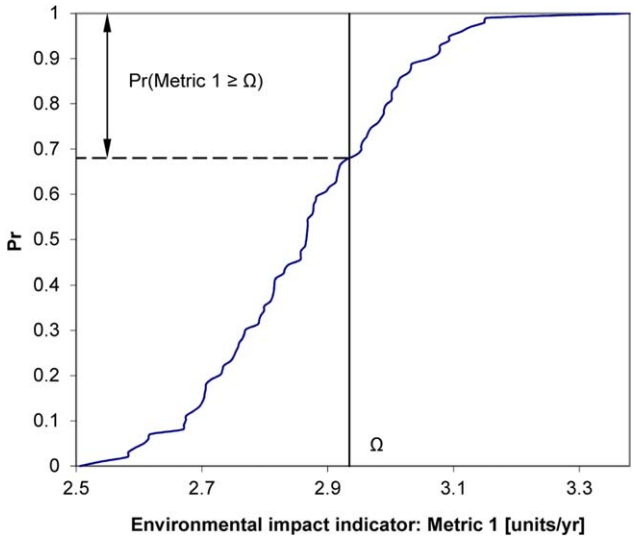

Figure 17. Cumulative probability curve for the design produced by the deterministic MINLP that maximizes the economic performance with an environmental limit of 2.93 units of Metric 1.

[Color figure can be viewed in the online issue, which is available at wileyonlinelibrary.com.]

solved first the deterministic MINLP, maximizing the economic performance and imposing an environmental limit Ω of 2.93 units on Metric 1 using a deterministic constraint. This environmental target corresponds to the value of the environmental impact in the maximum economic performance solution (see Figure 7 for further details). We then fixed the values of the decision variables (obtained from the deterministic MINLP) in the multiscenario MINLP (considering the uncertainty level and correlations of Case 1) and removed the environmental target limit on Metric 1. Figure 17 shows the cumulative probability curve of the deterministic solution. This solution was obtained following the procedure aforementioned. The curve is a visual representation of the cumulative probability function of the environmental impact indicator Metric 1. This figure indicates the probability at which the environmental impact of a solution will be less than or equal to a prespecified limit. To obtain this probability, we sort the scenarios in ascending order of their impact indicator values. To illustrate this, let us assume that we have four scenarios s1, s2, s3, and s4, with impacts i1, i2, i3, and i4, respectively. Let us further assume that these impacts are sorted in ascending orders follows: i3, i4, i1, and i2. Then, if the scenarios have all the same probability of occurrence, the cumulative probability of the impact indicator having a value less than or equal to i3 will be 0.25 (i.e., there is only one single scenario, s3, with an impact less than or equal to i3), 0.5 for i4 (i.e., two scenarios, s3 and s4, with an impact bellow or equal to i4), 0.75 for i1 (i.e., three scenarios, s3, s4, and s1, with an impact bellow or equal to i1), and 1.0 for i2 (i.e., all the scenarios with an impact less than or equal to i2).

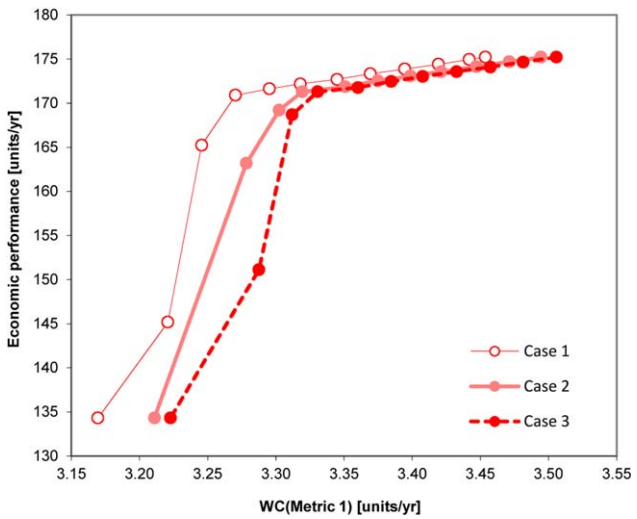

Figure 18. Pareto curves for Cases 1–3 displaying the trade-off between economic performance and WC values of Metric 1.

[Color figure can be viewed in the online issue, which is available at wileyonlinelibrary.com.]

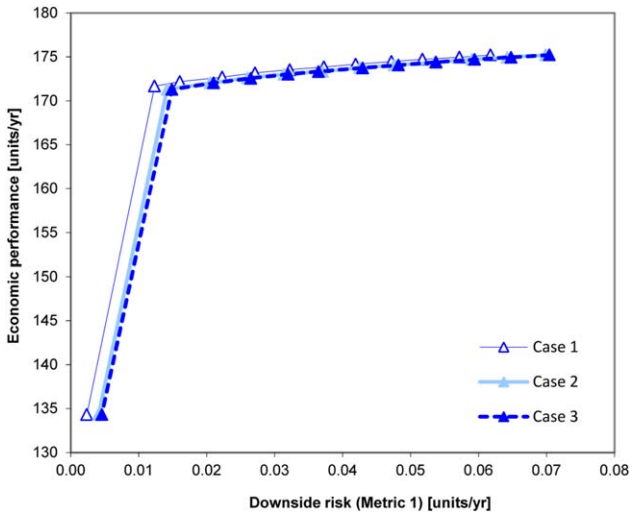

Figure 19. Pareto curves for Cases 1–3 displaying the trade-off between economic performance and downside risk values of Metric 1.

[Color figure can be viewed in the online issue, which is available at wileyonlinelibrary.com.]

As can be seen from Figure 17, the deterministic solution has about 32% chance of exceeding the environmental limit, even though the original solution was calculated for keeping the impact below this threshold. It is, therefore, clear that the deterministic MINLP may produce solutions that do not fully guarantee compliance with the desired environmental targets.

After highlighting the drawbacks of the deterministic approach, we next applied the stochastic MINLP for controlling the variability of Metric 1. To this end, we optimized the economic performance against each stochastic metric separately (i.e., WC and downside risk) for Cases 1, 2, and 3, which consider different degrees of correlation between emissions. The results obtained by running 12 iterations of the epsilon constraint method are shown in Figures 18 and 19. There is a clear trade-off between the economic and environmental performance under uncertainty in all of the cases. The WC metric and the downside risk metric both lead to Pareto fronts with two parts with different slopes separated by a knee (located in both cases close to an economic performance value of 172 units/yr).

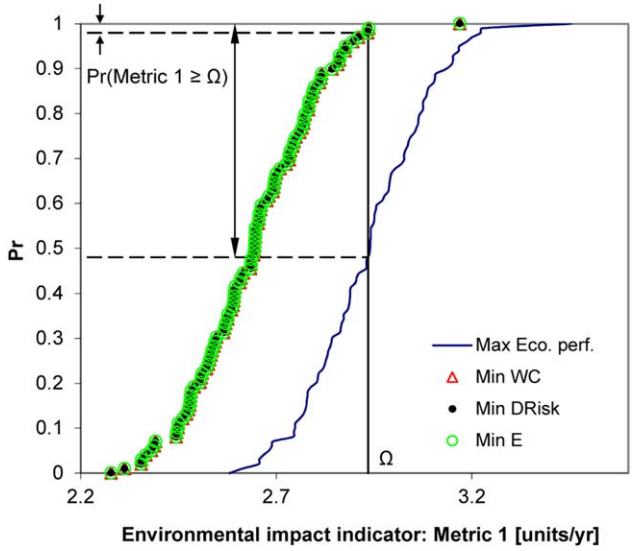

Figure 20. Cumulative probability curves for extreme solutions of Case 1.

[Color figure can be viewed in the online issue, which is available at wileyonlinelibrary.com.]

The Pareto fronts move rightward as the correlation between emissions increases (i.e., the environmental impact under uncertainty for a given economic performance level increases with larger correlations). This happens because in the correlated case the emissions that are correlated take simultaneously high values in some scenarios. In contrast, in the uncorrelated case, high emissions of one compound tend to be offset by low emissions of others, thereby avoiding scenarios with very large total emissions. Note that this effect is more pronounced when optimizing the WC metric as this metric is more sensitive to the presence of scenarios with very high emissions.

Figures 20–22 show the cumulative probability curves for Metric 1 in cases 1, 2, and 3, respectively. Each figure shows the probability of a value of Metric 1 when the WC is minimized, downside risk is minimized, and the expected value is minimized. In the same figure, we have depicted the cumulative probability curve of the deterministic solution, which is obtained by first minimizing the impact in the most likely scenario (i.e., considering the mean values of the uncertain parameters retrieved from Ecoinvent), and then recalculating the objective function by fixing the values of the decision variables in the stochastic MINLP. It is worthwhile to mention that the same solution could be ideally obtained by minimizing the expected impact in the stochastic MINLP for an infinite number of scenarios. For simplicity, we will refer from now on to the deterministic solution as the minimum expected impact solution as in principle both solutions should match for an infinite number of scenarios. The first thing to notice is that the minimization of the three environmental metrics (WC, DR, and expected impact) produces the same solution, and hence, the same probability curve. This curve lies entirely on the left-hand side of that associated with the maximum economic performance alternative, implying that the former solution will always show lower probabilities of surpassing the environmental limit independently of the environmental target of choice. For instance, in Case 1, the probability of exceeding the target of 2.93 is 0.52 for the maximum economic performance

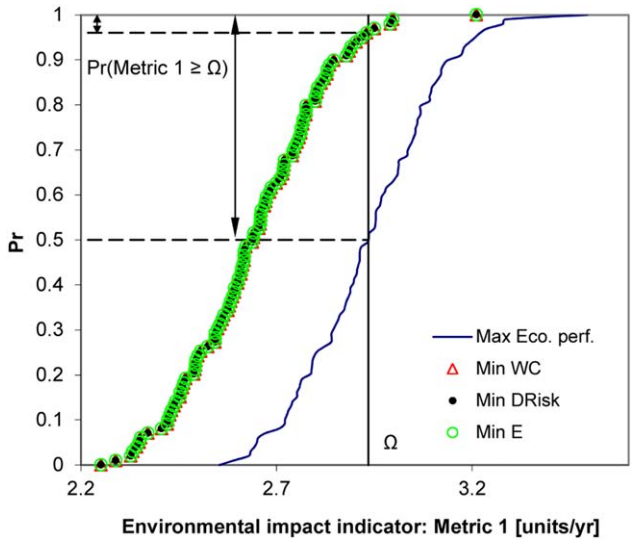

Figure 21. Cumulative probability curves for extreme solutions of Case 2.

[Color figure can be viewed in the online issue, which is available at wileyonlinelibrary.com.]

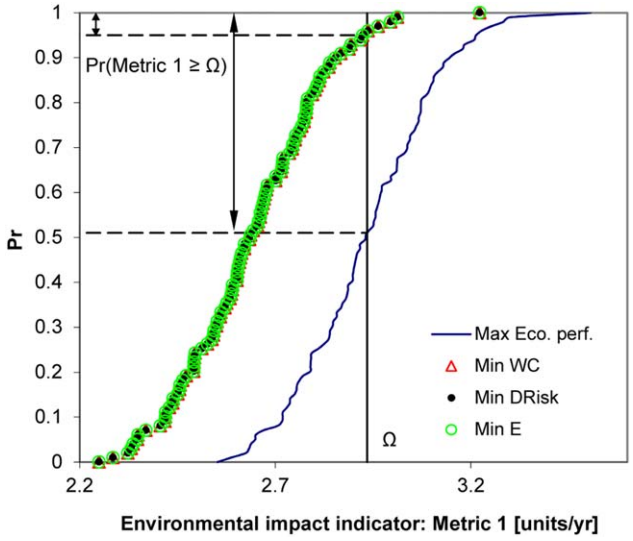

Figure 22. Cumulative probability curves for extreme solutions of Case 3.

[Color figure can be viewed in the online issue, which is available at wileyonlinelibrary.com.]

Table 7. Downside Risk, Worst Case and Economic Performance for Cases 1, 2 and 3

	Case 1	Case 2	Case 3
Maximum economic performance			
Downside risk Metric 1 (units/yr)	0.0618	0.0699	0.0705
Worst case Metric 1 (units/yr)	3.45	3.49	3.51
Economic performance (units/yr)	175.21	175.21	175.21
Minimum worst case			
Downside risk Metric 1 (units/yr)	0.0024	0.0041	0.0046
Worst case Metric 1 (units/yr)	3.17	3.21	3.22
Economic performance (units/yr)	134.32	134.32	134.32
Minimum downside risk			
Downside risk Metric 1 (units/yr)	0.0024	0.0041	0.0046
Worst case Metric 1 (units/yr)	3.17	3.21	3.22
Economic performance (units/yr)	134.32	134.32	134.32

solution, and only 0.02 in the minimum impact alternative. As observed, the cumulative curves widen with larger correlation coefficients. This is because the emissions that are correlated take simultaneously low/high values, thereby leading to extreme scenarios.

Table 7 displays the values of the WC, DR, and economic performance for the extreme solutions obtained in Cases 1, 2, and 3. As observed, we get larger values of the stochastic metrics as we increase the degree of correlation. In this particular case, and considering moderate uncertainty levels, we can see that both metrics (i.e., WC and DR) behave similarly, that is, their minimization lead to the same solution and when one is minimized the other is also decreased. Furthermore, these results demonstrate that correlations between emissions should be included in the analysis to avoid underestimation of the uncertainty effects. Note that these correlations cannot be accounted for using chance constraints, which was the approach followed in Guillén-Gosálbez and Grossmann.[37,38]

The flow sheet configuration of the maximum economic performance solution corresponds to that shown in Figure 8. The minimization of the WC and downside risk lead to flow sheets that are very similar to the minimum environmental impact solution produced by the deterministic MINLP. Similarly, as in the deterministic case, the model decides to replace fuel U1 by fuels U3 and U4, operate unit U8 and purchase R3 to reduce the environmental impact under uncertainty.

In the above cases, in which the uncertainty level is relatively small, both risk metrics lead to the same solution. A higher level of uncertainty in the parameters could lead to different solutions on using different metrics and further research is warranted on this issue. It is important that we address the uncertainty in the parameters to derive robust solutions as deterministic formulations are not able to capture the impact distributions.

Conclusions

In this article, we have proposed a systematic framework to handle uncertainties in the LCI data in MOO models that integrate LCA principles. The approach presented relies on a multiscenario stochastic MINLP in which the uncertain parameters are described by means of scenarios with equal probability of occurrence. These scenarios are generated taking into account the quality of the LCI data available. We evaluated two stochastic metrics: the downside risk and the WC.

We tested the capabilities of our approach using a complex industrial network and considering the uncertainty associated with the emissions due to the production of the main feedstock. It was shown that the deterministic MINLP produces solutions that exceed the desired environmental limits, when there is uncertainty in the data. Conversely, minimizing the WC and downside risk metrics lead to alternatives that minimize the probability of not meeting the environmental targets imposed by the decision-maker. Downside risk indicator accounts for both the probability of exceeding a given environmental limit and the deviation from such a limit. In contrast, the WC is rather sensitive to the existence of extreme scenarios, and could lead to solutions that minimize the environmental impact in the (very unlikely) worst scenario possible at the expense of economic performance. Numerical results also showed that it is important to account for correlations between emissions, as neglecting them may result in underestimation of the uncertainty effects.

Our tool can aid decision-makers and planners in multiple ways: (1) allow them to choose operating points from a set of Pareto solutions, (2) identify the main sources of environmental burdens, and (3) assess the effect of product constraints that influence economic performance and environmental impact. Future work will potentially focus on studying economic and environmental performance in other plausible scenarios (e.g., changing demands of products, costs etc.), analyzing the relative significance of different environmental metrics, and also on identifying redundant metrics that can be omitted from the analysis.

Acknowledgments

Financial support of this research work from the Spanish Ministry of Education and Science (projects CTQ2009-14420-C02), the Spanish Ministry of External Affairs (projects HS2007-0006 and A/023551/09), and the Generalitat de Catalunya (FI programs) is acknowledged.

Notation

Generic abbreviations

LCA = life-cycle assessment
MINLP = mixed-integer nonlinear programming
moMINLP = multiobjective mixed-integer nonlinear programming
MOO = multiobjective optimization
NL = variable that is not at its limiting value in an optimal solution (i.e., the constraint enforcing it is inactive and its Lagrangean multiplier is zero).
NLP = nonlinear programming
PSE = process systems engineering
R&D = Research and Development

Process abbreviations

C1–C7 = compounds
P1–P4 = final products
P5–P7 = byproducts
R1–R4 = raw materials
T1–T4 = final products storage tanks
T5–T7 = byproducts storage tanks
U1–U7 = utilities

Sets/Indices

B = set of environmental burdens indexed by b
C = set of scenarios indexed by c
E = set of impact categories indexed by e
I = set of units indexed by i
J = set of final products and byproducts indexed by j
K = set of raw materials indexed by k
MX_i = set of mixers associated with unit i (i.e., mixers whose output stream goes to unit i) indexed by mx
O = set of operating conditions indexed by o
P = set of properties indexed by p
S = set of streams indexed by s
SP_i = set of splitters associated with unit i (i.e., splitters whose main input stream comes from unit i) indexed by sp
U = set of utilities indexed by u

Subsets

$b \in DE$ = set of environmental burdens that are direct emissions
$b \in WA$ = set of environmental burdens that are waste materials
$i \in IM$ = set of units for which mass yields are defined
$i \in IR$ = set of units consuming raw material R2
$i \in I_u$ = set of process units that consume utility u
$i \in IV$ = set of units for which volume yields are defined
$o \in OI_i$ = set of operating conditions defined for unit i

$p \in PE$ = set of stream properties for which quality specifications are defined
$p \in PI$ = set of stream properties determined using Eq. 21 (i.e., as a weighted average on a volume basis and using the inverse of the property)
$p \in PM$ = set of properties determined using Eq. 20 (i.e., as a weighted average on a mass basis)
$p \in PS_s$ = set of properties defined for stream s
$p \in PT$ = set of properties determined using Eq. 22 (i.e., tailored correlations)
$p \in PV$ = set of properties determined using Eq. 19 (i.e., as a weighted average on a volume basis)
$s \in MS_i$ = main stream of unit i
$s \in SDE_b$ = set of direct emission streams that lead to environmental burden b
$s \in SFP$ = set of streams that are final products
$s \in SFP_j$ = set of streams containing product (or byproduct) j
$s \in SI_i$ = set of input streams to unit i
$s \in SI_{mx}$ = set of input streams to mixer mx
$s \in SI_{sp}$ = set of input streams to splitter sp
$s \in SO_i$ = set of output streams of unit i
$s \in SO_{mx}$ = set of output streams of mixer mx
$s \in SO_{sp}$ = set of output streams of splitter sp
$s \in SRMP_k$ = set of streams containing raw material k
$s \in SRMR_k$ = set of streams containing raw material k that are recycled from other process units
$s \in SWA_b$ = set of waste streams that lead to environmental burden b
$u \in U_i$ = set of utilities consumed by unit i

Continuous variables

$\tilde{IMP}_e$ = damage in impact category e when uncertainties are present
$\tilde{ENVI}$ = Stochastic total environmental impact of the process
$\tilde{LCI}_b$ = life-cycle inventory entry associated with emission, feedstock requirements or waste b when uncertainties are present
COSTS = process total cost associated with the purchase of raw materials and the consumption of utilities
DRisk = downside risk
ECOP = economic performance of the process
ENVI = deterministic total environmental impact of the process
F_s = volume flow rate of stream s
GR_s = density of stream s
IMP_e = damage in impact category e in the deterministic case
LCI_b = life-cycle inventory entry associated with emission, feedstock requirements or waste b in the deterministic case
M_s = mass flow rate of stream s
$OPC_{i,o}$ = operating condition o of unit i
$PROP_{s,p}$ = property p of stream s
REV = Revenues from the process
$RMCONS_{i,s}$ = flow rate of stream s input into unit i
$RMCONS_i^{MASS}$ = consumption of raw material R2 in unit i on a mass basis
$RMCONS_i^{VOL}$ = consumption of raw material R2 in unit i on a volume basis
RMCOSTS = cost of purchases of raw materials consumed in the process
$TCONS_u$ = total amount of utility u consumed
$UTCONS_{i,u}$ = consumption rate of utility u in unit i
UTCOSTS = cost of utilities consumed in the process WC value
$YIELD_{i,s}^{MASS}$ = yield of output stream s of unit i on mass basis
$YIELD_{i,s}^{VOL}$ = yield of output stream s of unit i on volume basis
$YIELDS_{i,s}$ = yield of output stream s of unit i (expressed either on a mass or volume basis, $YIELD_{i,s}^{MASS}$ and $YIELD_{i,s}^{VOL}$, respectively)
δ_c = auxiliary value for calculating the downside risk

Binary variables

Y_i = 1 if fuels of type 1 (U1 and U2) are selected in unit i, and 0 if fuels U3 or U4 are chosen instead
Z_c = Binary variable (1 if the impact in scenario c is above the target limit, 0 otherwise)

Parameters

$\omega_{b,s}^{RM}$ = LCI entry associated with burden b (i.e., an emission, waste generated or feedstock) generated per unit of raw material in stream s consumed in deterministic case
$\omega_{b,u}^{UT}$ = LCI entry associated with burden b(i.e., an emission, waste generated or feedstock) generated per unit of utility u consumed in deterministic case
$\tilde{\omega}_{b,s}^{RM}$ = LCI entry associated with burden b (i.e., an emission, waste generated or feedstock) generated per unit of raw material in stream s consumed when uncertainties are present
$\tilde{\omega}_{b,u}^{UT}$ = LCI entry associated with burden b (i.e., an emission, waste generated or feedstock) generated per unit of utility u consumed when uncertainties are present
BM = Large parameter
CAP_i^{MASS} = Mass capacity of unit i
CAP_i^{VOL} = Volume capacity of unit i
$COST_k^{RM}$ = Unitary cost of raw material k
$COST_k^{UT}$ = Unitary cost of utility u
D_s = Demand of final/intermediate product contained in stream s
$DSAT_s$ = Minimum demand satisfaction level (in percentage %) of final product in stream s
$ECONS_i$ = Energy consumption coefficient linking the energy consumed by unit i to the volumetric flow rate of the main input stream to i
M = Large parameter
$PRICE_j$ = Unitary selling price of product/byproduct j
$prob_c$ = Probability of scenario c
$PROP_{s,p}^{LO}$ = Lower bound on property p of final product contained in stream s
$PROP_{s,p}^{UP}$ = Upper bound on property p of final product contained in stream s
TOP = Total number of operating hours
$UTRATE_{i,u}$ = Mass-balance coefficient linking the amount of utility u consumed by unit i to the volumetric flow rate of the main input stream to i
$X_{s,b}$ = Fraction of environmental burden (direct emission or waste) b in stream s
$\theta_{b,e}$ = Damage factor that translates burden b (i.e., an emission, waste generated or feedstock) into the corresponding environmental damage in impact category e
Ω = Environmental performance target

Literature Cited

1. Grossmann IE, Guillén-Gosálbez G. Scope for the application of mathematical programming techniques in the synthesis and planning of sustainable processes. *Comput Chem Eng*. 2010;34(9):1365–1376.
2. Guinée JB, Gorée M, Heijungs R, Huppes G, Kleijn R, de Koning A, van Oers L, Wegener Sleeswijk A, Suh S, Udo de Haes HA, de Bruijn H, van Duin R, Huijbregts MAJ. *Handbook on Life Cycle Assessment. Operational Guide to the ISO Standards*. Dordrecht: Kluwer Academic Publishers, 2002.
3. Azapagic A, Clift R. The application of life cycle assessment to process optimisation. *Comput Chem Eng*. 1999;10:1509–1526.
4. Guillen-Gosalbez G, Caballero J, Jimenez L. Application of life cycle assessment to the structural optimization of process flowsheets. *Ind Eng Chem Res*. 2008;47(3):777–789.
5. Stefanis SK, Livingston, AG, Pistikopoulos, EN. Environmental impact considerations in the optimal design and scheduling of batch processes. *Comput Chem Eng*. 1997;21:1073–1094.
6. Pistikopoulos E, Stefanis S. Optimal solvent design for environmental impact minimization. *Comput Chem Eng*. 1998;22(6):717–733.
7. Eliceche AM, Corvalán SM, Martínez P. Environmental life cycle impact as a tool for process optimisation of a utility plant. *Comput Chem Eng*. 2007;31(5–6):648–656.
8. Papandreou V, Shang Z. A multi-criteria optimisation approach for the design of sustainable utility systems. *Comput Chem Eng*. 2008; 32(7):1589–1602.
9. Gebreslassie BH, Guillén-Gosálbez G, Jiménez L, Boer D. Design of environmentally conscious absorption cooling systems via multi-objective optimization and life cycle assessment. *Appl Energy*. 2009; 86(9):1712–1722.
10. Gebreslassie BH, Guillén-Gosálbez G, Jiménez L, Boer D. A systematic tool for the minimization of the life cycle impact of solar assisted absorption cooling systems. *Energy*. 2010;39(9):3849–3862.

11. Liu P, Pistikopoulos EN, Li Z. A multiobjective optimization approach to polygeneration energy systems design. *AIChE J*. 2010; 56(5):1218–1234.
12. Hugo A, Pistikopoulos EN. Environmentally conscious long-range planning and design of supply chain networks. *J Clean Prod*. 2005; 13:1471–1491.
13. Mele F, Espuña A, Puigjaner L. Environmental impact considerations into supply chain management based on life-cycle assessment. In: LCM 2005 International Conference on Innovation by Life Cycle Management, Barcelona (Spain), 2005.
14. Puigjaner L, Guillén-Gosálbez G. Towards an integrated framework for supply chain management in the batch chemical process industry. *Comput Chem Eng*. 2008;32(4–5):650–670.
15. Pozo C, Ruíz-Femenia R, Caballero J, Guillén-Gosálbez G, Jiménez, L. On the use of Principal Component Analysis for reducing the number of environmental objectives in multi-objective optimization: application to the design of chemical supply chains. *Chem Eng Sci*. 2012;69(1):146–158.
16. Bojarski A, Lainez JM, Espuna A, Puigjaner L. Incorporating environmental impacts and regulations in a holistic supply chains modeling: an LCA approach. *Comput Chem Eng*. 2009;33(10):1747–1759.
17. Hugo A, Rutter P, Pistikopoulos S, Amorelli A, Zoia G. Hydrogen infrastructure strategic planning using multi-objective optimization. *Int J Hydrogen Energy*. 2005;30(15):1523–1534.
18. Guillén-Gosálbez G, Mele F, Grossmann IE. A bi-criterion optimization approach for the design and planning of hydrogen supply chains for vehicle use. *AIChE J*. 2010;56:650–667.
19. Mele F, Kostin A, Guillén-Gosálbez G, Jimenez L. Multiobjective model for more sustainable fuel supply chains. A case study of the sugar cane industry in Argentina. *Ind Eng Chem Res*. 2011;50(9): 4939–4958.
20. Bernardi A, Giarola S, Bezzo F. Optimizing the economics and the carbon and water footprints of bioethanol supply chains. *Biofuels Bioprod Bioref*. 2012;6(6):656–672.
21. Pieragostini C, Mussati MC, Aguirre P. On process optimization considering LCA methodology. *J Environ Manage*. 2012;96(1):43–54.
22. Sahinidis, NV, Optimization under uncertainty: state-of-the-art and opportunities. *Comput Chem Eng*. 2004; 28(6–7):971–983.
23. Aseeri A, Bagajewicz MJ. New measures and procedures to manage financial risk with applications to the planning of gas commercialization in Asia. *Comput Chem Eng*. 2004;28(12);2791–2821.
24. Heijungs R. Part I: a general framework for the analysis of uncertainty and variability in life cycle assessment. *Int J Life Cycle Assess*. 1998;3(5):273–280.
25. Reap J, Roman F, Duncan S, Bras B. A survey of unresolved problems in life cycle assessment. Part 2: impact assessment and interpretation. *Int J Life Cycle Assess*. 2008;13(5):374–388.
26. Hoffman L, Weidema BP, Kristiansen K, Ersboll AK. *Statistical Analysis and Uncertainties In Relation to LCA*. Special Reports No. 1. Conpenhagen, Denmark: Nordic Council of Ministers, 1995.
27. Chevalier JL, Le Téno JF. Life cycle analysis with ill-defined data and its application to building products. *Int J Life Cycle Assess*. 1996;1(2):90–96.
28. Beccali G, Beccali M, Cellura M. *Fuzzy Set Application in Life Cycle Inventory of Building Materials*. In: Proceedings of the Second International Conference on Building and the Environment. Volume 1: Assessment methods and natural resources. Paris, France: Centre Scientifique et Technique du Bâtiment, 1997.
29. Petersen EH. Life-Cycle *Assessment of Building Components. Handling Uncertainties in LCAs*. In: Proceedings o the Second International Conference on Building and the Environment. Volume 1: assessment methods and natural resources. Paris, France: Centre Scientifique et Technique du Bâtiment, 1997.
30. Kennedy DJ, Montgomery DC, Quay BH. Data equality. Stochastic environmental life cycle assessment modelling. A probabilistic approach to incorporating variable input data quality. *Int J Life Cycle Assess*. 1996;1(4):199–207.
31. Capello C, Hellweg S, Badertsecher B, Hungerbüler K. Life-Cycle Inventory of waste solvent distillation: statistical analysis of empirical data. *Environ Sci Technol*. 2005;39:5885–5892.
32. Geisler G, Hellweg S, Hungerbühler K. Uncertainty analysis in life cycle assessment (LCA): case study on plant-protection products and implications for decision making. *Int J Life Cycle Assess*. 2005; 10(3):184–192.
33. Sugiyama H, Fukushima Y, Hirao M, Hellweg S, Hungerbühler K. Using standard statistics to consider uncertainty in industry-based Life Cycle Inventory databases. *Int J Life Cycle Assess*. 2005;10(6): 399–405.
34. Van Zelm R, Huijbregts MAJ, Posthuma L, Wintersen A, Van De Meent D. Pesticide ecotoxicological effect factors and their uncertainties for freshwater ecosystems. *Int J Life Cycle Assess*. 2009; 14(1):43–51.
35. Hung ML, Ma HW. Quantifying system uncertainty of life cycle assessment based on Monte Carlo simulation. *Int J Life Cycle Assess*. 2009;14(1):19–27.
36. Ruiz-Femenia R, Guillén-Gosálbez G, Jiménez L, Caballero JA. Multi-objective optimization of environmentally conscious chemical supply chains under demand uncertainty. *Chem Eng Sci*. 2013;95:1–11.
37. Guillén-Gosálbez G, Grossmann, IE. Optimal design and planning of sustainable chemical supply chains under uncertainty. *AIChE J*. 2009;55(1):99–12.
38. Guillén-Gosálbez G, Grossmann, I. A global optimization strategy for the environmentally conscious design of chemical supply chains under uncertainty in the damage assessment model. *Comput Chem Eng*. 2010;34(1):42–58.
39. Ben-Tal A, Nemirovski A. Robust convex optimization. *Math Oper Res*. 1998;23(4):769–805.
40. Janak SL, Lin X, Floudas CA. A new robust optimization approach for scheduling under uncertainty. II. Uncertainty with known probability distribution. *Comput Chem Eng*. 2007;31(3):171–195.
41. Barbaro A, Bagajewicz M. Managing financial risk in planning under uncertainty. *AIChE J*. 2004;50(5):963–989.
42. Eppen GD, Martin RK, Schrage L. A scenario approach to capacity planning. *Oper Res*. 1989;37(4):517–527.
43. Weidema BP, Wesnæs MS. Data quality management for life cycle inventories—an example of using data quality indicators. *J Clean Prod*. 1996;4:167–174.
44. Law AM, Kelton WD. *Simulation Modeling and Analysis*, *3rd ed*. New York: McGraw Hill, 2000.
45. Haimes YY, Lasdon LS, Wismer DA. On a bi-criterion formulation of the problems of integrated system identification and system optimization. *IEEE Trans Syst Man Cybern 1*. 1971:296–297.
46. Ehrgott M. *Multicriteria Optimization*, 2nd ed. Springer, Berlin (Germany), 2000.
47. Grossmann IE. Review of nonlinear mixed-integer and disjunctive programming techniques. *Optim Eng*. 2002;3:227–252.
48. Althaus H, Doka G, Dones R, Heck T, Hellweg S, Hischier R, Nemecek T, Rebitzer G, Spielmann M, Wernet G. *Ecoinvent Report No. 1*. Technical Report, Swiss Centre for Life Cycle Inventories, Dübendorf (Switzerland), 2007.
49. Brooke A, Kendrick D, Meeraus A, Raman R. *GAMS—A User's Manual*. Washington, DC: GAMS Development Corporation, 1998.

Manuscript received April 17, 2013, and revision received Oct. 7, 2013.